JOURNAL OF ENZYME INHIBITION AND MEDICINAL CHEMISTRY
2023, VOL. 38, NO. 1, 2270781
https://doi.org/10.1080/14756366.2023.2270781

Taylor & Francis
Taylor & Francis Group

REVIEW ARTICLE

OPEN ACCESS Check for updates

Latest advances in dual inhibitors of acetylcholinesterase and monoamine oxidase B against Alzheimer's disease

Dajiang Zou[a], Renzheng Liu[a], Yangjing Lv[a], Jianan Guo[a], Changjun Zhang[a] and Yuanyuan Xie[a,b,c]

[a]College of Pharmaceutical Science, Zhejiang University of Technology, Hangzhou, China; [b]Collaborative Innovation Center of Yangtze River Delta Region Green Pharmaceutical, Zhejiang University of Technology, Hangzhou, China; [c]Key Laboratory for Green Pharmaceutical Technologies and Related Equipment of Ministry of Education, Key Laboratory of Pharmaceutical Engineering of Zhejiang Province, Hangzhou, China

ABSTRACT

Alzheimer's disease (AD) is a progressive brain disease characterised by progressive memory loss and cognition impairment, ultimately leading to death. There are three FDA-approved acetylcholinesterase inhibitors (donepezil, rivastigmine, and galantamine, AChEIs) for the symptomatic treatment of AD. Monoamine oxidase B (MAO-B) has been considered to contribute to pathologies of AD. Therefore, we reviewed the dual inhibitors of acetylcholinesterase (AChE) and MAO-B developed in the last five years. In this review, these dual-target inhibitors were classified into six groups according to the basic parent structure, including chalcone, coumarin, chromone, benzo-fused five-membered ring, imine and hydrazine, and other scaffolds. Their design strategies, structure-activity relationships (SARs), and molecular docking studies with AChE and MAO-B were analysed and discussed, giving valuable insights for the subsequent development of AChE and MAO-B dual inhibitors. Challenges in the development of balanced and potent AChE and MAO-B dual inhibitors were noted, and corresponding solutions were provided.

ARTICLE HISTORY
Received 7 August 2023
Revised 15 September 2023
Accepted 27 September 2023

KEYWORDS
Alzheimer's disease; AChE inhibitors; MAO-B inhibitors; dual inhibitors

Introduction

AD is a brain disorder hallmarked with intracellular neurofibrillary tangles (NFTs) and extracellular β-amyloid (Aβ) deposits, which induces progressive memory loss and cognitive dysfunction, afflicting over 50 million people worldwide and posing a tremendous threat on the health of the elderly[1–3]. Although many hypotheses have been proposed and studied in the process of investigating AD[4], and some milestone discoveries have been made[5], the pathological mechanism of AD is still unclear. The cholinergic system, as a primary neurotransmitter system, has been successfully applied in the development of anti-AD drugs. Several AChEIs successively approved by U.S. Food and Drug Administration (FDA) were the primary drugs for AD therapy (Figure 1)[6,7]. Furthermore, increasing evidence indicated that the peripheral anion site (PAS) of AChE was believed to induce Aβ aggregation neurotoxicity, providing a prospect for the development of AChE-based multifunctional anti-AD agents[8].

The amine homeostasis in the brain was affected by the oxidative deamination of monoamine oxidase (MAO), which was a flavin-containing enzyme present in the outer membrane of mitochondria. MAO could be classified into two types, MAO-A and MAO-B[9,10]. Recently, the MAO-B has been found to be overexpressed in the hippocampus and cerebral cortex of AD patients[11]. Moreover, various neurotoxic byproducts produced in MAO-B catalysed biochemical reactions would further induce mitochondrial dysfunction and neuronal death[12,13], implying that MAO-B inhibitors can provide beneficial neuroprotective effects for AD therapy by increasing monoamine neurotransmitters and reducing the production of the reactive oxygen species (ROS)[14].

Considering the complexity of AD pathology, the "one drug, one target" paradigm could not achieve the desired therapeutic effects[15]. However, the multi-target-directed ligands (MTDLs) strategy, a single multifunctional molecule that could modulate multiple interconnected pathologic pathways, could be an effective way to alter the course of the disease[16,17]. This approach was thought to be more advantageous than combination therapy because it not only maintained the multiple pharmacodynamics of combination therapy, but also added some additional benefits, such as avoiding potential risks caused by drug-drug interactions, lower risk of adverse effects, and a simplified dosing regimen, which improved compliance[18].

Multifunctional molecules were obtained through three rational design approaches: linkage, fusion, and incorporation (Figure 2). The linkage approach connecting two prototype molecules through a linker was simple to implement and could be applied in structurally incompatible molecular scaffolds. But with the increase in molecular size, this approach might lead to poor drug-like properties including solubility, blood-brain barrier (BBB) permeability, and bioavailability. The fusion approach directly combined two scaffolds without a linker, and the incorporation approach was applied by integrating or overlapping scaffolds[18–21]. Despite there might be disadvantages and challenges, the MTDLs strategy was still most favourable in terms of multifactorial diseases.

CONTACT Yuanyuan Xie xyycz@zjut.edu.cn; Changjun Zhang zhangchangjun@zjut.edu.cn College of Pharmaceutical Science, Zhejiang University of Technology, Hangzhou 310014, China

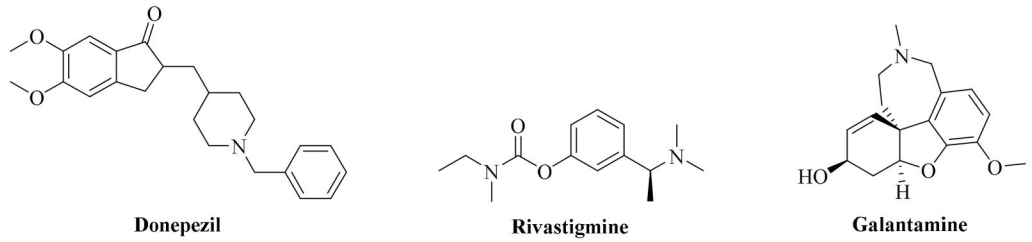

Figure 1. AChEIs approved by the FDA for AD therapy.

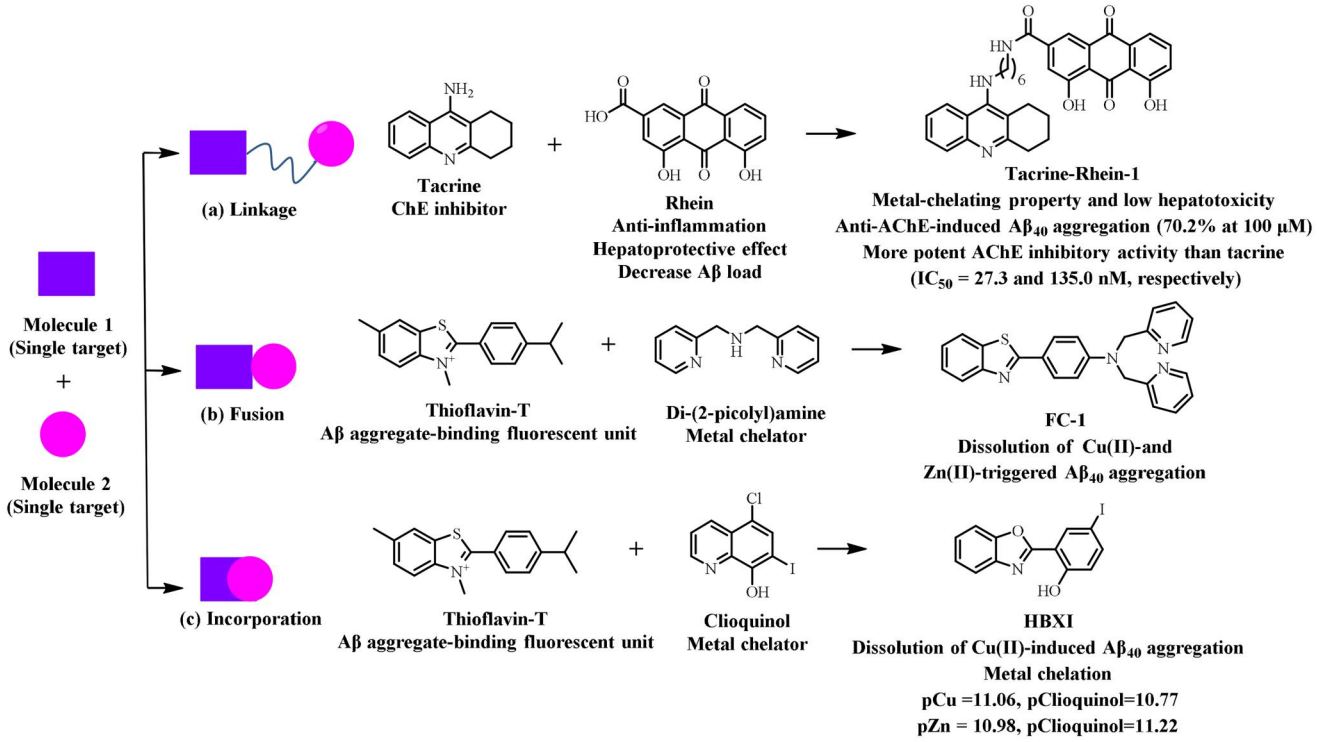

Figure 2. Three rational design strategies to generate multifunctional molecules.

As the first AChE inhibitor approved for AD therapy, tacrine had been widely applied in MTDLs strategy to obtain potent AChEIs with additional pharmacological benefits[22]. Previous study revealed that Rhein possessed hepatoprotective, anti-Aβ aggregation, and metal-chelating activities. The potent candidate tacrine-rhein-1 was synthesised by Liu et al.[23] using the linkage approach, and exhibited greater activity against AChE compared to tacrine (IC_{50} = 27.3 and 135.0 nM, respectively). Tacrine-rhein-1 could bind to Cu^{2+} and inhibit the Aβ aggregation induced by AChE (70.2% at 100 μM). Notably, compared to tacrine, lower levels of aspartate aminotransferase and alanine aminotransferase were observed in mice serum after administration of tacrine-rhein-1, indicating lower hepatotoxicity.

Given that Aβ aggregation and ROS production induced by metal ions were two significant neurotoxic events in AD[24], and metal-induced Aβ aggregation was reversible[25], thus, chelation therapy by administration of metal-specific chelating ligands seemed to be a reasonable choice for the treatment of AD[26]. Thioflavin-T, a fluorescent dye binding to Aβ, and metal chelator di(2-picolyl)amine were chosen to synthesise FC-1 through the fusion approach[25]. As expected, FC-1 was not only capable of inhibiting the $A\beta_{40}$ aggregation but also resulting in the dissociation of $Cu^{2+}$and Zn^{2+}-triggered $A\beta_{40}$ aggregates. Rodríguez-Rodríguez et al.[27] chose the incorporation approach of integrating the features of thioflavin-T and clioquinol to synthesise a multifunctional candidate HBXI that could inhibit Cu^{2+}-promoted $A\beta_{40}$ aggregation and efficiently chelate Cu^{2+} (pCu = 11.06, pClioquinol = 10.77) and Zn^{2+} (pZn = 10.98, pClioquinol = 11.22) ions.

Therefore, in recent years, the concept of AChE/MAO-B dual inhibitors has gained significant interest for the treatment of AD[28], and numerous AChE and MAO-B dual inhibitors designed using MTDLs strategy have been well-documented. In particular, several novel techniques played an important role in the discovery of new hit inhibitors.

In recent years, nanotechnology, especially magnetic nanoparticles (MNPs), has been widely applied in immobilisation due to their unique properties. Immobilising important enzymes onto nanoparticles can provide comprehensive benefits[29]. In this context, the Zhang group[30] employed AChE-immobilized MNPs as a tool to screen AChEIs from natural products and found an amentoflavone, which displayed more potent AChE inhibition (IC_{50} = 0.73 μM) than tacrine. Li and colleagues[31] created a non-conjugated polymer dots (NCPDs)-MnO_2 biosensing system to screen AChEIs, which exhibited a broader detection range (12.3–3675 U L^{-1} for AChE), and an impressive low limit of detection (LOD) at 4.9 U L^{-1}, showing a promising prospect in the discovery of new AD therapy drugs.

Computer-aided drug design (CADD) has become an indispensable tool for discovering lead compounds and providing useful

structural information of receptor-ligand complexes for subsequent research[32]. Zhou group[33] discovered a well-known natural product kaempferol as an AChE inhibitor, while another group[34] identified this compound as a selective human MAO-A inhibitor. Gogineni et al.[35] adopted this strategy to enhance the selectivity of flavonoid acacetin 7-*O*-methyl ether, resulting in a thousand-fold increase of the selectivity index for MAO-B. In addition, Wang group[36] adopted the Three-Dimensional Biologically Relevant Spectrum (BRS-3D), a representative compound database used in CADD, to evaluate the subtype selectivity of MAO inhibitors, observing a thousand-fold selectivity index improvement for MAO-B.

Light irradiation has extensive application in the field of disease treatment such as the Photodynamic therapy (PDT)[37], a therapeutic method for various cancers. Interestingly, Paolino et al.[38] designed a small library of AChE and MAO-B dual inhibitors that could modify their activity through light irradiation, representing a novel exploration in the design of dual inhibitors. In summary, these novel techniques expedite lead compound discovery and expand the pool of potential candidates for AD treatment.

This review provided a summary and discussion of AChE and MAO-B dual inhibitors published from 2018 to 2022, including the design strategies employed, the SARs, molecular docking studies, the challenges faced and corresponding solutions.

The AChE and MAO-B binding sites

As a serine hydrolase, AChE was extensively distributed in the peripheral and central nervous system and was responsible for hydrolysing acetylcholine (ACh)[39]. AChE was an ellipsoidal protein with dimensions of approximately 45 Å × 60 Å × 65 Å. It possessed a deep and narrow gorge (∼20 Å) formed by 14 aromatic residues (e.g. Ser200, Phe289, Tyr121, and Gly199) consisting of two binding sites, known as the PAS and the catalytic anionic site (CAS)[40]. The PAS guided ACh into the CAS site through the "cation-π" interaction, and ACh was subsequently hydrolysed at the CAS site[41].

MAO-B was responsible for catalysing the metabolism of monoamine neurotransmitters, and one of its key binding sites was the flavin adenine dinucleotide (FAD)[14]. The binding pocket of MAO-B (∼700 Å^3) was divided into the entrance cavity and substrate cavity by the Ile199 and Tyr326 residues[42]. The flexible Ile199 residue was pivotal in controlling the entry of ligands into the enzyme cavity[43–45]. In addition, a smaller hydrophobic entrance cavity, lined with specific residues Tyr398 and Tyr435, was adjacent to the substrate cavity, could generate an "aromatic cage", interacting with the amino group of the substrate through π-cation interactions[44,46].

AChE and MAO-B dual inhibitors

The fundamental principle for designing AChE and MAO-B dual inhibitors was to incorporate the pharmacophores of anti-AD molecules or drugs (Figure 3). For example, the cholinesterase (ChE) inhibitory moiety of donepezil was amalgamated into the potent MAO-B inhibitor PF9601N to create the lead ASS234, which was further modified to obtain a highly stable candidate Contilisant in human liver microsomes. The carbamate group of rivastigmine was merged into potent MAO-B inhibitors M30 and rasagiline, synthesising the M30D and Ladostigil, respectively[47–50]. In particular, Ladostigil displayed a brain-selective inhibitory profile on MAO in an *in vivo* study. When administered to mice (26 mg·kg^{-1}) for two weeks, it resulted in approximately 70% inhibition of brain MAO activity, but there was almost no MAO inhibition in the liver and small intestine[51]. This unique advantage enabled it to avoid side effects caused by cheese reactions during the treatment of AD[52]. Recently, a Phase III clinical trial of Ladostigil to treat mild cognitive impairment (MCI) suggested that the combination of AChE and MAO-B inhibitors is a promising treatment for AD[53].

Chalcone-based inhibitors

Chalcone, a compound found in many plants, is composed of two benzene rings separated by three carbon atoms[54]. In this paper, the aromatic ring connected to the carbonyl group is named the A ring, while the other benzene ring is defined as the B ring. Chalcone and its analogs have attracted great interest for decades on account of their diverse pharmacological properties such as antitumor, anti-inflammatory, anti-diabetic, antioxidant, and antimicrobial agents[55]. In particular, certain natural and synthesised chalcone derivatives (Figure 4) exhibited both AChE and MAO-B inhibitory activities.

Oh et al.[56] reported that compouds **1**, **2**, **4**, **5**, and **6** exhibited moderate AChE inhibitory activities (IC_{50} = 2.79, 1.25, 6.07, 6.02, and 2.46 μM, respectively) and potent MAO-B inhibitory effects (IC_{50} = 0.082, 0.066, 0.029, 0.061 and 0.075 μM, respectively). But compound **3** showed weak activity against both enzymes (IC_{50} = 31.30 and 10.06 μM, respectively). This difference was attributed to the formation of hydrogen bonds between Cys172 of MAO-B (PDB: 4A79) with **1, 2, 4, 5,** and **6**, but not with **3**, probably due to the steric hindrance and possible charge effect caused by the carboxymethyl group. Interestingly, **3** displayed weaker AChE inhibition despite forming a hydrogen bond with AChE (PDB: 1GQS) Phe288, which was not observed in **1, 2, 4, 5,** and **6**. In addition, the inhibitory activities of both enzymes decreased or disappeared when the 2′ position of the A ring was substituted with methoxy (**7**, **8**)[46], ethoxy (**9**)[57], morpholine (**10**)[58] or piperazinyl (**11**)[59] groups due to the blocked interaction between the A ring and two enzymes.

Furthermore, both inhibitory activities decreased sharply (**12**)[60] when the A ring underwent cyclisation using a benzothiazine ring, while AChE inhibitory activity significantly increased when the A ring was cyclized by 1, 3-dioxolane and the B ring was replaced by thiophene ring (**13**)[61] (Figure 5). These observations could be explained through docking studies of **13**. The 1,3-benzodioxole ring established π–π interactions with Tyr72 and Trp286 of AChE (PDB: 4EY7), and Tyr326 of MAO-B (PDB: 2V5Z), a hydrogen bond with Tyr188 of MAO-B, respectively. Additional π–π interactions were observed between the thienyl ring and Tyr341 of both AChE and MAO-B.

Chalcone and donepezil-based dual inhibitors

Donepezil has been extensively investigated in the development of multifunctional anti-AD candidates for its good bioavailability, high selectivity, and low toxicity (Figure 6). In light of this, several moderate and balanced dual inhibitors of AChE and MAO-B were synthesised by Sang et al. [62] *via* a linkage approach. Compound **14** showed potent AChE inhibitory activity (IC_{50} = 0.41 μM) with moderate MAO-B inhibitory activity (IC_{50} = 8.8 μM). Moreover, it revealed antioxidant and metal chelate abilities. A docking study revealed that **14** interacted with AChE (PDB: 1EVE) through hydrogen bonds and π–π interactions established between its hydroxyl, methoxy groups with Arg289, Tyr334. Besides, an important intermolecular hydrogen bond was found between the *N*-(2-

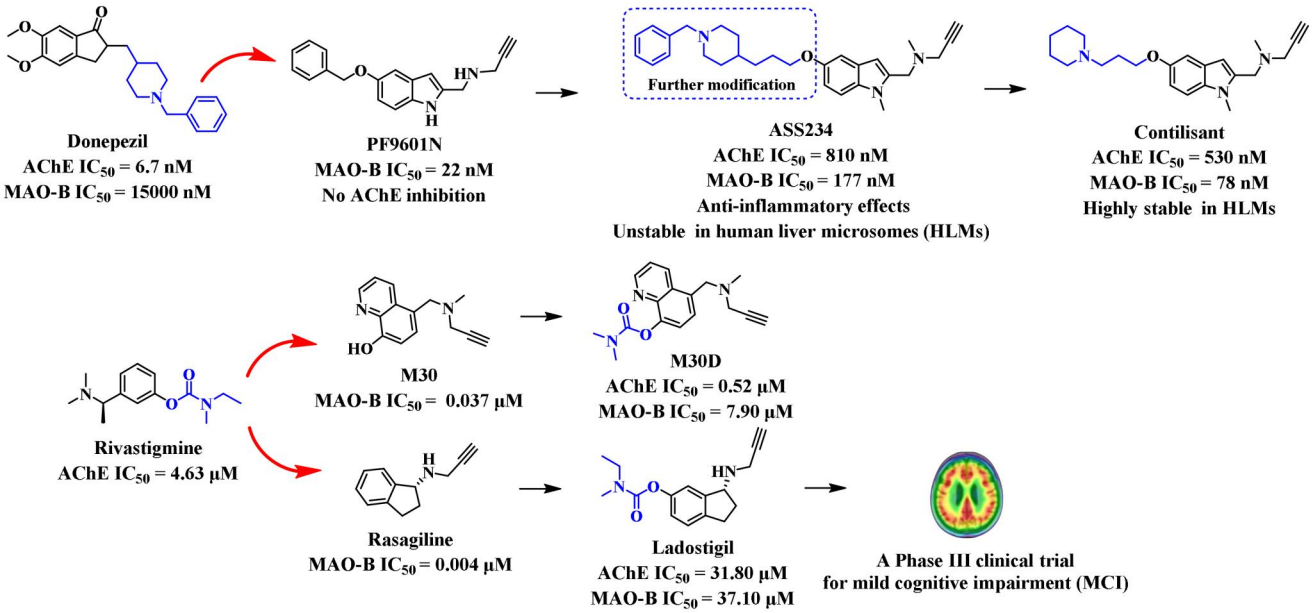

Figure 3. Structures of promising MTDLs.

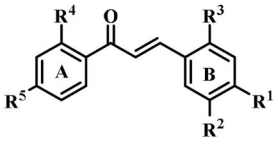

1 R^1=Cl, R^2=R^3=R^4=R^5=H
2 R^1=NO_2, R^2=R^3=R^4=R^5=H
3 R^1=CH_2COOH, R^2=R^3=R^4=R^5=H
4 R^1=$N(CH_3)_2$, R^2=R^3=R^4=R^5=H
5 R^1=$N(CH_3)_2$, R^2=R^3=R^4=H, R^5=Cl
6 R^1=$N(CH_3)_2$, R^2=R^4=H, R^3=R^5=Cl
7 R^1=R^5=OH, R^2=R^3=H, R^4=OMe
8 R^1=R^2=R^5=OH, R^3=H, R^4=OMe
9 R^1=R^2=R^3=R^4=H, R^5=OC_2H_5
10 R^1=R^2=R^3=R^4=H, R^5=morpholine
11 R^1=R^2=R^3=R^4=H, R^5=piperazinyl

Compounds	IC_{50} (μM)	
	AChE	MAO-B
1	2.79 ± 0.11	0.082 ± 0.0016
2	1.25 ± 0.42	0.066 ± 0.0025
3	31.30 ± 1.65	10.06 ± 3.44
4	6.07 ± 0.17	0.029 ± 0.0028
5	6.02 ± 0.04	0.061 ± 0.0021
6	2.46 ± 0.078	0.075 ± 0.0028
7	> 40	0.38 ± 0.023
8	25.01 ± 1.03	1.01 ± 0.12
9	> 50	0.57 ± 0.030
10	12.07 ± 1.18	0.32 ± 0.16
11	No inhibition	1.37 ± 0.0027

Figure 4. Structures of natural and synthesised chalcone.

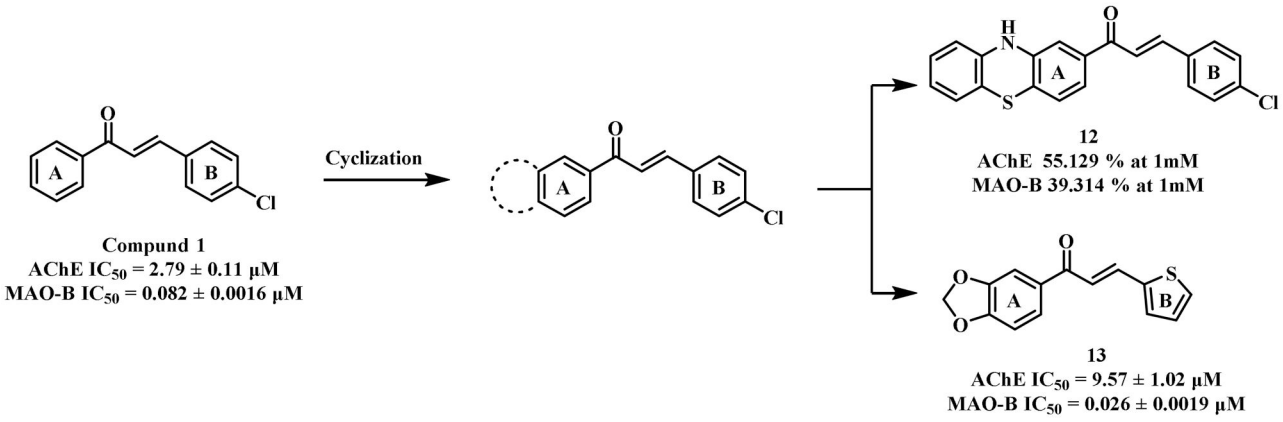

Figure 5. Structures of compound 1-based derivatives.

methoxybenzyl) ethylamine fragment and Ser122. In addition, several intermolecular hydrogen bonds (e.g. between the methoxyl group and Ala325) were also observed between the **14** and MAO-B (PDB: 2V60).

To develop improved anti-AD candidates, **15** and **16** were synthesised by the same research group using a linkage approach[63,64]. As expected, these compounds displayed more balanced AChE (IC_{50} = 0.13 and 1.3 μM, respectively) and MAO-B

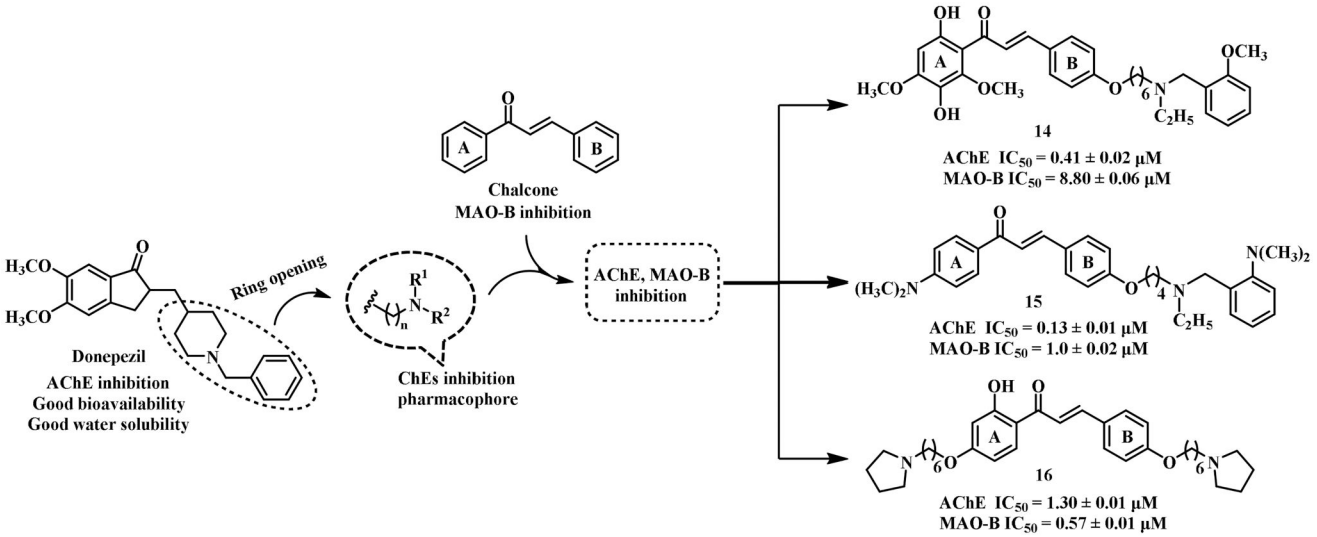

Figure 6. Structures of chalcone and donepezil-based dual inhibitors.

inhibitory activity (IC_{50} = 1.0 and 0.57 μM, respectively), along with excellent anti-self-induced Aβ aggregation and potent antioxidant abilities. What's more, **15** revealed no neurotoxicity (1000 mg·kg^{-1}) in mice, and demonstrated improvement in memory impairment induced by scopolamine. The 2-(dimethylamino)-*N*-ethyl-benzenemethanamine moiety of **15** could enter into the CAS and interact with AChE (PDB: 4EY7) Trp286. A hydrogen bond was formed between the hydroxyl group on the A ring and Tyr314, and π–π interactions were established between the A ring and Trp286, as well as Tyr341. In addition, hydrophobic interactions were also observed with several AChE residues (e.g. Tyr337, Trp286, and Trp86). The 2-hydroxy-acetophenone moiety of **15** generated two hydrogen bonds with Phe168, and Cys172 of MAO-B (PDB: 2V60). Additionally, the aromatic rings (A and B rings of chalcone) established π–π interactions with Leu171 and Tyr435 of MAO-B. These interactions were likely resposible for the MAO-B inhibitory activity exhibited by **15**. Compound **16** fully occupied the pocket of AChE (PDB: 1EVE), with the A ring forming a π–π interaction with Phe330. The oxygen atom of the B ring formed an intermolecular hydrogen bond with Phe288. In addition, the hydroxyl group generated two hydrogen bonds with Ile198, and Gln206 of MAO-B (PDB: 2V60), respectively. The carbonyl moiety generated hydrogen bonds with Ile199 and Cys172, and the B ring also established π–π interactions with MAO-B residues, Tyr398 and Tyr435.

Other chalcone-based dual inhibitors

Compound **17**, synthesised by Sang et al.[65] using the fusion approach, is a carbamate derivative of chalcone. Unfortunately, It showed no significant AChE inhibition (26.2 ± 0.89% at 25 μM), but moderate MAO-B inhibition (IC_{50} = 1.3 ± 0.06 μM) in *in vitro* biological test. In the molecular docking study of **17**, limited interactions between **17** and AChE (PDB: 1EVE) were observed, which was consistent with its extremely weak AChE inhibitory activity. However, it was observed that the hydroxyl and carbonyl groups formed hydrogen bonds with two key residues Ile199 and Tyr326 of MAO-B (PDB: 2V60), respectively. Moreover, the oxygen atom and carbonyl group of the carbamate fragment established hydrogen bonds with Tyr398.

Phenolic Mannich bases have demonstrated various neuroprotective effects including antioxidant[66], AChE inhibition[67], and metal chelation[68]. Most importantly, the conversion of these bases into ammonium salts resulted in better solubility[69]. In light of this, several research groups created a series of chalcone-polyphenol Mannich bases using the fusion approach (Figure 7). Compound **18** exhibited balanced inhibitory activity against the target enzymes, with an IC_{50} value of 7.15 μM for AChE and 0.43 μM for MAO-B70. In the *Torpedo californica* AChE (*Tc*AChE)-**18**-complex (PDB: 1EVE), the phenylacetate group occupied the PAS by forming a key hydrogen bond with Ser286, and the protonated piperidine fragment bound to the CAS through a hydrogen bond and salt bridge with Asn85 and Asp72, respectively. In addition, the chalcone skeleton could bind to the mid-gorge through π–π interaction with residues such as Tyr334. On the other hand, in the docking study of MAO-B (PDB: 2V5Z), the 3′-OH on the B ring of **18** established a hydrogen bond with Gly101 and the piperidine moiety formed a salt bridge with Glu84. Moreover, the A ring occupied the entrance cavity and interacted with the key residue Ile199, while a π–π interaction was also found in the substrate cavity between the phenyl at 4-position and Tyr398.

Another structurally simplified chalcone-Mannich base derivative **19** demonstrated similar AChE and MAO-B inhibitory potency (IC_{50} = 0.44 and 1.21 μM, respectively)[71]. In addition, it exhibited antioxidant activity, the ability to inhibit Aβ aggregation and metal-chelating properties. The molecular modelling study revealed that **19** could interact simultaneously with the two binding sites (CAS and PAS) of AChE (PDB: 1EVE). The carbonyl moiety and 3′-OH group generated hydrogen bonds with Tyr435 and Ile199 of MAO-B (PDB: 2V60), respectively. Furthermore, A ring established a π–π interaction with Tyr398.

Drugs containing oxime ether fragments are widely administrated for various diseases, including antibiotic, antifungal, and anti-inflammatory. Oh et al.[72,73] synthesised a series of chalcone oxime ethers using the fusion approach and evaluated their inhibitory potency on AChE and MAO-B (Figure 7). Among them, compound **20** exhibited the most balanced inhibitory against both enzymes (IC_{50} = 4.39 and 0.028 μM, respectively), and displayed superior MAO-B inhibitory potency compared to the positive drug lazabemide (IC_{50} = 0.042 μM). Simplification of the oxime ether moiety in compound **21** led to **a** significant decrease in AChE inhibitory potency (6.3% at 10 μM), but a slight increase in MAO-B inhibitory potency (IC_{50} = 0.012 μM). A similar result was observed when the A ring of chalcone was decorated with the dioxime ether (**22**, 11.2% at 10 μM for AChE; IC_{50} = 0.018 μM

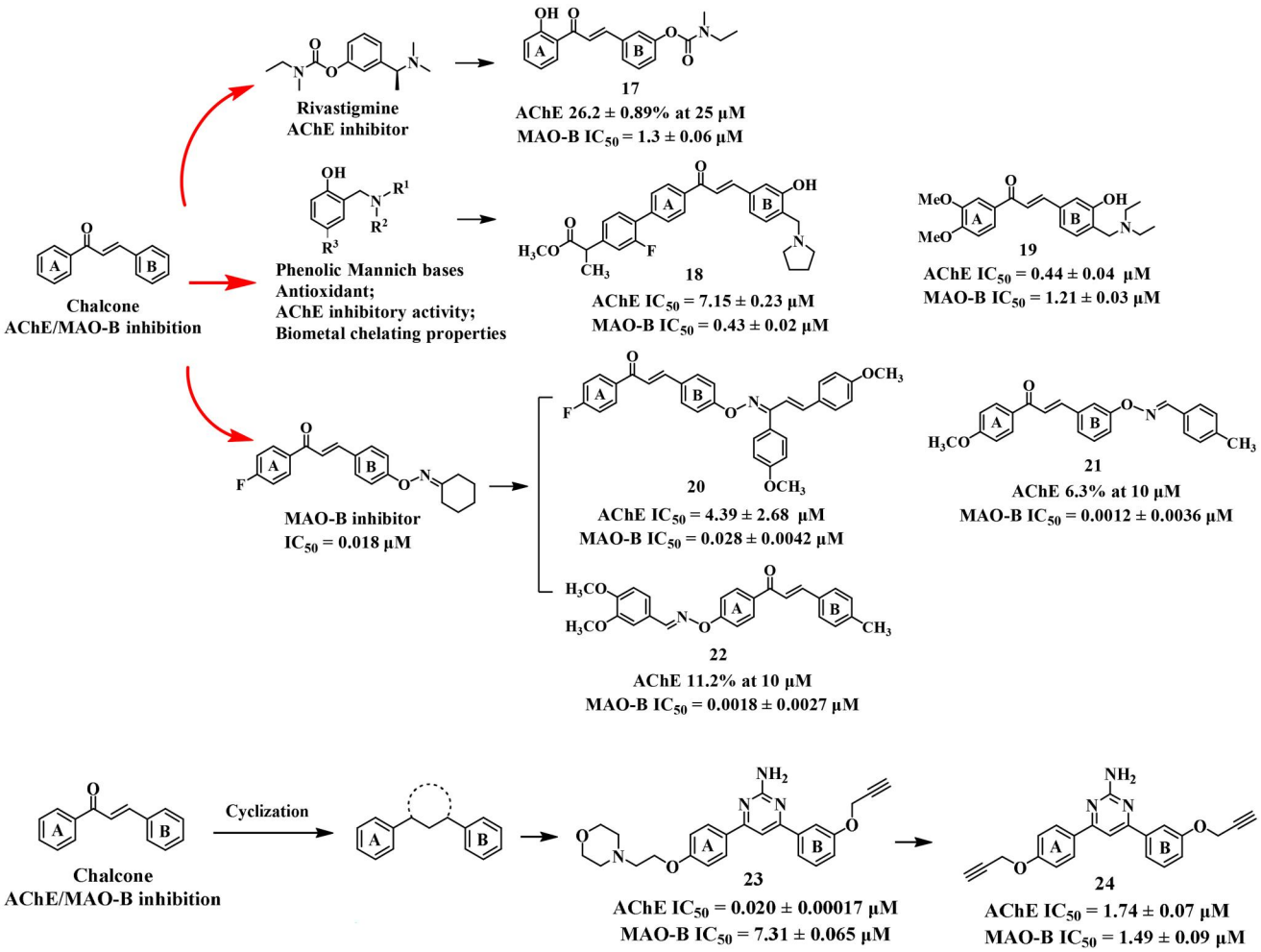

Figure 7. Structures of other chalcone-based dual inhibitors.

for MAO-B). In the molecular docking studies, these chalcone oxime ethers could interact with the aromatic cage composed of FAD, Tyr435, and Tyr398, while the B ring established π–π interaction with the MAO-B (PDB: 2V5Z) selective residue Tyr326.

In an earlier study by Kumar's team[74], they developed novel pyrimidine derivatives as multi-target anti-AD agents by cyclizing the three-carbon fragment of chalcone using the incorporation approach. Most of them exhibited potent selective AChE inhibition, but weak inhibitory potency on MAO-B (e.g. **23**, IC_{50} = 0.020 μM and 7.31 μM, respectively). To enhance the inhibitory potency on MAO-B of these compounds, the morpholine moiety was replaced with propargyl group[75]. However, *in vitro* assays showed that the optimised compound exhibited only a slightly increase in inhibitory potency against MAO-B, but a dramatic decrease in AChE inhibitory activity (**24**, IC_{50} = 1.49 and 1.74 μM, respectively), suggesting that the morpholine moiety was indispensable for the potent AChE inhibitory activity.

3.1.3. Summary of SARs

Based on the SARs of chalcone derivatives (Figure 8), the AChE inhibitory activities decrease with the substitution of hydroxyl, alkoxy groups at 2-position, morpholine, piperazine groups or oxime ether moiety at the 4-position of A ring. Meanwhile, the cyclisation of A ring into a 10*H*-phenothiazine scaffold with greater rigidity also leads to decreased AChE inhibitory activity. Additionally, the substitution with a hydroxyl group at the 4′-position, or carbamate or oxime ether moieties at the 3′-position of B ring results in the decrease of AChE inhibitory activities. Conversely, the AChE inhibitory activities increase when the substitution with chlorine, *N,N*-dimethylamino or aminoalkyl groups at the 4′-position of B ring. The MAO-B inhibitory potency increases when substituted with oxime ether moiety or propargyl group at the 4-position of A ring, or chlorine, nitro groups at the 4′-position of B ring. Conversely, the MAO-B inhibitory activity decreases when substituted with morpholine, or piperazine groups at 4-position at A ring. Substitution with the oxime ether moieties in the B ring does not significantly affect MAO-B inhibitory activities. The substitution of the carboxymethyl group at the 4′-position of ring B was disadvantageous for both AChE and MAO-B inhibition. In addition, the cyclisation of the carbonyl group of chalcone yields potent and balanced AChE and MAO-B dual inhibitors. The AChE inhibitory activities is determined by crucial residues such as Arg289, Ser122, Tyr314, Phe330, and Trp286 of AChE, which facilitate the A ring of chalcones to bind to the middle gorge and CAS through hydrogen bonds or π–π stacking interactions. Other important residues, including Trp286, Phe288, and Tyr341 in the PAS, can interact with the B ring *via* the π–π interactions. In addition, the α,β-unsaturated carbonyl group can form hydrogen bonds with specific residues. On the other hand, MAO-B inhibitory activities are influenced by the residues Ile199, Cys172, Tyr 435, Tyr326, and Tyr398 of MAO-B, which enable the chalcone derivatives to enter the active pockets by forming hydrogen bonds and π–π interactions.

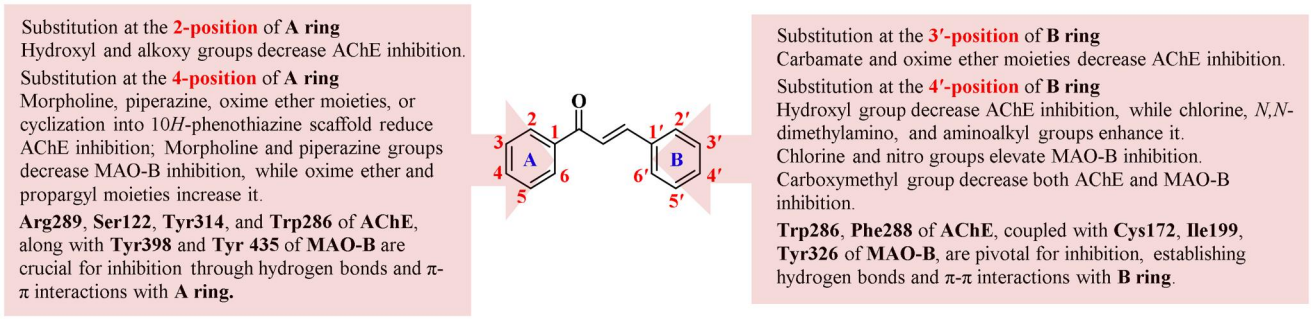

Figure 8. SAR of chalcone-based dual inhibitors targeting AChE and MAO-B.

Coumarin-based inhibitors

Coumarins, characterised by 1,2-benzopyranone or benzopyran-2-one, are widely found in various plants. Studies have demonstrated that natural coumarins and synthesised analogs exhibit anti-AChE and MAO-B activities[76–81]. Coumarins have been reported to bind to PAS of AChE, suggesting their potential in designing and synthesising new analogs with excellent and balanced AChE and MAO-B inhibitory activities. As a result, numerous dual inhibitors targeting both enzymes have been developed by incorporating coumarin core with some catalytic site interacting moieties.

Modifications at position 3 or 4 of coumarin

Structural decoration at position 3 or 4 of coumarin has been a significant strategy to develop effective AChE and MAO-B inhibitors (Figure 9). In previous studies, representative compounds **25** and **26,** modified on the 3 position of coumarin bearing an amide linker by using the linkage approach, showed weak AChE inhibition (IC_{50} = 591.44 and 69.47 μM, respectively), but remarkable MAO-B inhibition at the nanomolar level (IC_{50} = 4.6 and 760 nM, respectively)[82,83]. However, **27** and **28** displayed potent and balanced inhibitory activities against both AChE and MAO-B (IC_{50} = 0.163 and 0.068 μM for AChE; 8.13 and 6.31 μM for MAO-B, respectively) when alkylamine served as the linker[84], suggesting that the alkylamine linker is more advantageous for developing coumarin-based dual inhibitors targeting these enzymes.

Rehuman et al.[85] synthesised a series of coumarin-chalcone compounds using the fusion approach to introduce α,β-unsaturated ketone unit of chalcone at the 3 position of coumarin and evaluated their AChE and MAO-B inhibitory potencies. Among them, **29** displayed weak AChE inhibiton (IC_{50} = 40.1 μM), but potent MAO-B inhibitory activity with an IC_{50} value of 0.51 μM. The weak AChE inhibitory activity might be due to the inability of **29** to reach the CAS centre of AChE (PDB: 4EY7) and interact with Trp82.

In addition, Zhang *et al*. also modified the 4 position of coumarin using the linkage approach to obtain the representative compound **30**, which showed effective AChE inhibition with an IC_{50} value of 0.84 μM, but displayed weak MAO-B inhibitory potency (IC_{50} = 12.31 μM)[84].

Modification at position 7 of coumarin

In most studies, the focus has been on designing dual inhibitors targeting AChE and MAO-B by using the linkage approach to introduce moieties at position 7 of coumarin, which bound to the CAS site (Figure 9). However, when an amide linker was used as the connecting group, the inhibitory activity of the compounds against AChE and MAO-B was not balanced, as observed with **31** and **32**[86]. When an aromatic amide was substituted at position 7 of coumarin, **31** showed no significant AChE inhibition (45–50% at 100 μM), while the MAO-B inhibitory activity of compound **32** was almost disappeared (IC_{50} > 100 μM) when fatty amide was decorated at the same position. This could be attributed to the inability of **31** and **32** to simultaneously bind to the active sites of both AChE and MAO-B.

On the other hand, **33**[87]**, 34**[88]**, 35** and **36**[89], displayed potent and balanced activity against both enzymes (IC_{50} = 0.55, 0.114, 1.3, and 1.4 μM for AChE, respectively; IC_{50} = 0.0082, 0.101, 0.051 and 0.076 μM for MAO-B, respectively) when the CAS binding groups were introduced at the position 7 of coumarin through a flexible alkyl ether linker. Molecular docking studies have shown that these molecules occupied the active sites of the target enzyme and interacted with key residues of AChE (PDB: 4EY7) such as Trp286, Tyr341, Trp86, Tyr337, Gly448, His447, and Gly121. Meanwhile, the coumarin core was accommodated within the substrate cavity of MAO-B (PDB: 2V61) and established interactions with residues such as Tyr398, Phe343, Tyr60, and Tyr435. The carbonyl moiety of coumarin formed hydrogen bonds with residues such as Tyr188. Other fragments of these compounds were observed to occupy the entrance cavity of MAO-B and interacted with residues including Pro102, Pro104, and Ile316.

Summary of SARs

Coumarin is an extremely valuable skeleton for the discovery and development of highly potent AChE and MAO-B dual inhibitors. SARs of coumarin derivatives, as shown in Figure 10, reveal that substitution with benzylamine derivatives at the 3- or 4-position of the coumarin scaffold can significantly improve the AChE inhibitory activities. AChE inhibitory activities decrease sharply if the benzylamine groups at the 3-position of the coumarin core are replaced with benzamide moieties, but MAO-B inhibitory activities can be remarkably increased. The introduction of α,β-unsaturated ketone moiety at the 3-position of the coumarin core reduces the AChE inhibitory activities of coumarin derivatives. Substitution with benzamide moieties at the 7-position of the coumarin core makes it difficult to obtain balanced AChE and MAO-B dual inhibitors. On the contrary, the introduction of flexible AChE inhibitory pharmacophores at the same 7-position of coumarin is advantageous for obtaining potent and balanced AChE and MAO-B dual inhibitors. Furthermore, the presence of the *N*-benzylpiperidine or *N*-alkyloxy moiety at the 7-position of the coumarin has no significant effect on the AChE inhibition, but exhibited a remarkable impact on the MAO-B inhibition, suggesting that decoration of the protonatable portion has a greater influence on MAO-B affinity compared to AChE.

The Trp286 in AChE PAS plays an important role in interacting with the coumarin core through a π–π interaction. While, residues Trp86, His447, and Gly121 in AChE CAS interact with the protonatable basic moieties through cation-π interactions. The Tyr188 at

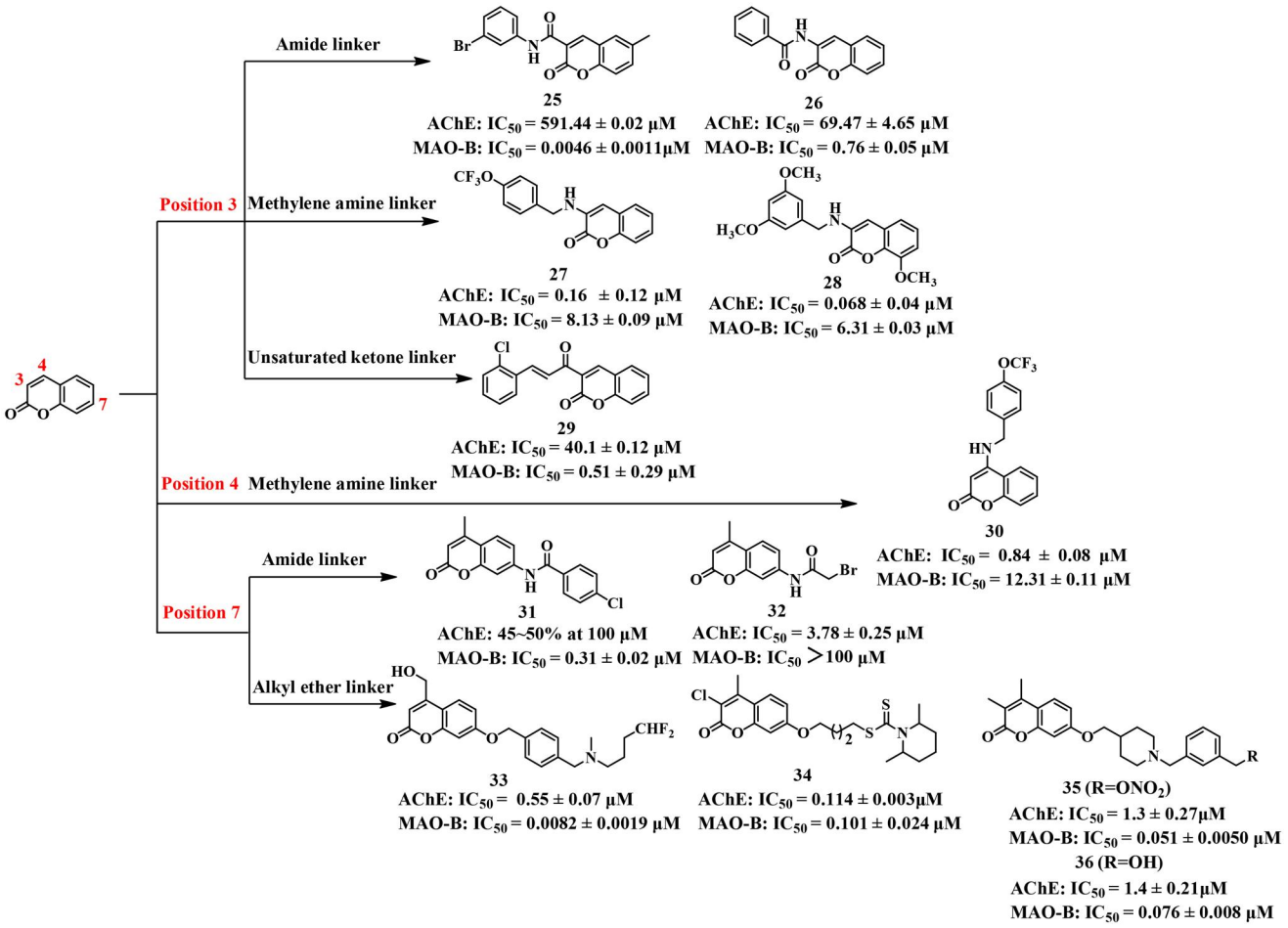

Figure 9. Structures of coumarin-based inhibitors.

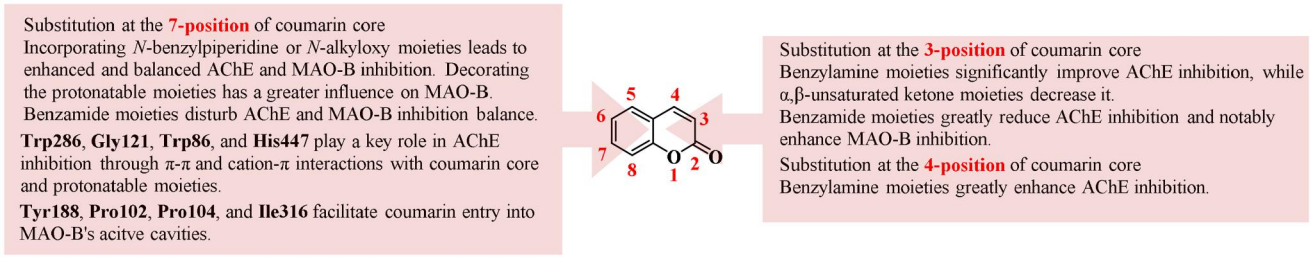

Figure 10. SAR of coumarin-based dual inhibitors targeting AChE and MAO-B.

the bottom of the substrate cavity of MAO-B can form a hydrogen bond with the carbonyl oxygen of the coumarin, and certain residues (e.g. Tyr398, Tyr435) stabilise coumarins by establishing hydrophobic interactions. Additionaly, residues Pro102, Pro104, and Ile 316 enable coumarins to enter into the entrance cavity of MAO-B.

Chromone-based inhibitors

3.3.1. Modification of chromones

Chromone (4*H*-chromen-4-one), an isomer of coumarin (2*H*-chromen-2-one), is a kind of significantly important scaffold due to its potential for modification, generating chromone derivatives with diverse biological activities. For instance, compounds **37** and **38** (Figure 11) displayed potent MAO-B inhibitory activity, and were synthesised by the introducing carboxyl group onto the chromone core[90]. The screening results showed that the position of the carboxyl group is critical for the selectivity of MAO inhibitors. Compound **37**, with the carboxyl group substituted at position 3 of the chromone core, displayed selective MAO-B inhibition with an IC_{50} value of 48 nM (SI >2083) due to a crucial hydrogen bond established between the carboxyl group and Tyr326. However, isomer **38,** with the same carboxyl substitution at position 2, showed weaker MAO-B inhibitory potency (IC_{50} > 100 nM). Therefore, previous studies[91,92] have used the linkage approach to develop selective MAO-B inhibitors (e.g. **39–41**) featured a carboxylamide linker substitution at the 3-position of the chromone core. However, recent studies have focused on the synthesis of numerous chromone derivatives to obtain multifunctional anti-AD lead compounds (Figure 11).

By using the fusion approach to introduce AChE inhibitory pharmacophores, two compounds (**42** and **43**) bearing carboxamide substitution at position 3 of chromone were synthesised, and their inhibitory activities against the target enzymes were

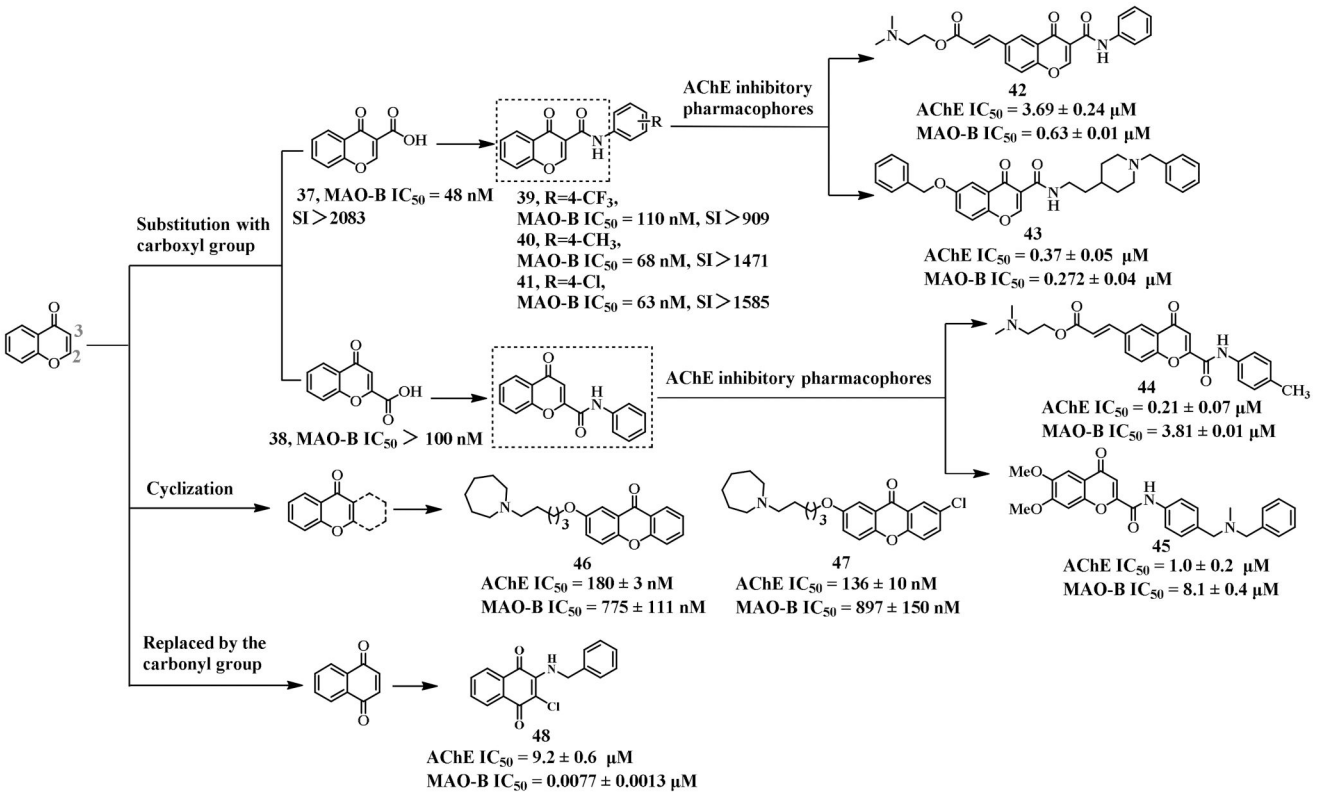

Figure 11. Structures of chromone-based inhibitors.

evaluated[93,94]. Both compounds were AChE and MAO-B dual inhibitors, but compared to **42** (IC_{50} = 3.69 μM), **43** displayed more potent AChE inhibitory activity (IC_{50} = 0.37 μM), suggesting that the *N*-benzylpiperidine moiety, serving as the pharmacophore of AChEIs, might be more noteworthy in the design of AChE and MAO-B dual inhibitors. Furthermore, **43** was proved to cross the BBB and show safety on rat pheochromocytoma (PC12) cells. Docking studies of **43** revealed that the π-cation and π–π interactions were generated between the *N*-benzylpiperidine moiety and Trp84, as well as Phe330 in CAS of AChE (PDB: 1EVE). Additionally, the chromone fragment established π–π interaction with Trp279 in PAS. In the case of MAO-B (PDB: 2V60), the benzyloxy moiety established π–π interactions with Tyr435 and Tyr398, while the amide carbonyl group formed a hydrogen bond with Tyr326. In contrast, the *N*-benzylpiperidine fragment was located in the entrance cavity.

Interestingly, compared to **42**, using the fusion approach, dual inhibitor **44** showed more potent AChE inhibitory activity (IC_{50} = 0.21 μM), but weaker MAO-B inhibitory potency (IC_{50} = 3.81 μM) when the carboxamide linker was substituted at position 2 of chromone core[93]. In addition, compound **45** obtained using the fusion approach with carboxamide group substituted on the same position of chromone core, displayed balanced inhibition towards both enzymes with IC_{50} values of 1.0 and 8.1 μM, respectively[95]. This indicated that the introduction of AChE inhibitory moieties, specifically when the carboxamide group was substituted at position 2 of the γ-pyrone nucleus, may lead to a dual inhibitor with stronger AChE inhibitory activity.

Łażewska et al.[96] synthesised potent dual inhibitors **46** (IC_{50} = 180, and 775 nM, respectively) and **47** (IC_{50} = 136, and 897 nM, respectively) using the incorporation approach to cyclize the chromone skeleton. The docking studies indicated that the azepane rings interacted with His440, Trp84 and Phe330 of AChE (PDB: 1EVE). Moreover, the *N* atoms established hydrogen bonds with a crucial water molecule 1159, and the alkyl moiety generated hydrophobic interactions with several residues such as Phe330, and Phe290. On the other hand, the xanthone core was located in PAS, and engaged π–π and hydrophobic interactions with several residues (e.g. Tyr334, Tyr70, Tyr121, and Trp279). In addition to the cyclisation of the chromone skeleton, the balanced AChE and MAO-B inhibitor **48** (IC_{50} = 9.2 and 0.0077 μM, respectively) with anti-Aβ_{40} aggregation (IC_{50} = 3.2 μM), was obtained by using the incorporation approach to substitute the *O* atom of pyranone with the carbonyl group[97]. Docking studies demonstrated that the naphthoquinone core interacted with Trp286 of AChE (PDB: 4EY7) via π–π interaction, while the carbonyl group bound to Tyr72 and Tyr124 by hydrogen bonds. On the other hand, the carbonyl groups established three hydrogen bonds with Tyr326, Tyr435, and Gln206 of MAO-B (PDB: 6FWC). In addition, an intriguing halogen bond was observed between the chlorine atom of **48** and Cys172 of MAO-B.

Summary of SARs

Chromone, as a significant scaffold, is widely found in numerous natural products and synthetic compounds, exhibiting a wide range of biological activities. SARs of chromone-based inhibitors are shown in Figure 12. By introducing AChE inhibitory pharmacophores onto the chromone scaffold bearing formamide group as linker at 3-position of chromone core, balanced dual inhibitors of AChE and MAO-B are created. Substitution with formamide moiety at 2-position of chromone core, and introduction of AChE inhibitory pharmacophores onto the 6-position of chromone can increase the AChE inhibitory activities, but decrease MAO-B inhibitory potencies. Introduction of donepezil-like pharmacophores at 2-position of chromone core using formamide moiety as linker leads to a decrease in both AChE and MAO-B inhibitory activities. Furthermore, if donepezil-like pharmacophores are introduced at

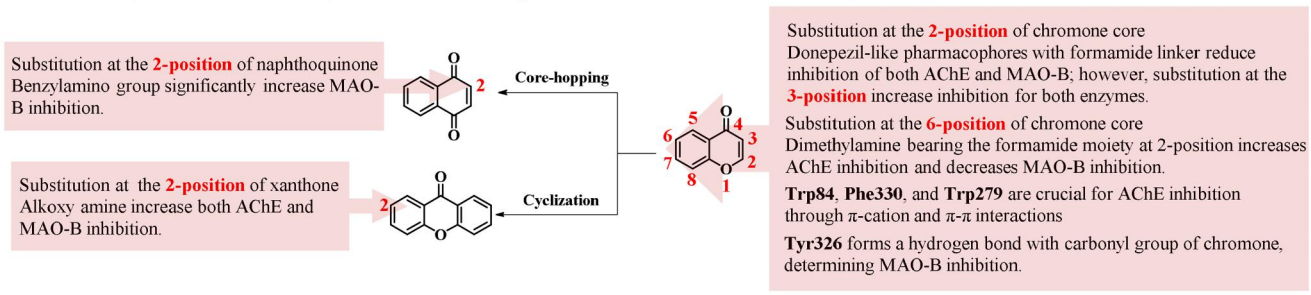

Figure 12. SAR of chromone-based dual inhibitors targeting AChE and MAO-B.

the 3-position of the chromone core, both AChE and MAO-B inhibitory activities increase. Additionally, the chromone nucleus is easily modifiable, allowing for the acquisition of novel scaffolds (xanthone and naphthoquinone) by cyclisation or core-hopping strategies. The introduction of flexible alkoxy amine at the 2-position of xanthone results in AChE and MAO-B inhibitory activities increased. Similarly, the benzylamino group at the 2-position of naphthoquinone significantly enhances the MAO-B inhibitory activity.

Docking studies indicated that residues Trp84, and Phe330 in CAS, Trp279 in PAS were important factors in determining the AChE inhibitory activities of chromone derivavtives by forming π-cation and π–π interactions. While, residues Tyr435, Tyr398, and Tyr326 of MAO-B played an important role in the MAO-B inhibitory activities by establishing π–π interactions or hydrogen bound.

Benzo five-membered ring-based inhibitors

Heteroaromatic compounds, including benzofuran, benzothiophene, indole, and others, are essential organic compounds found in nature. These compounds serve as common structural units in many bioactive molecules, and have wide applications in medicine, dyes, agriculture, new materials and other fields[98]. As a result, studies of these compounds have gained increasing attention, particularly in the field of pharmaceutical chemistry (Figure 13).

Compound **49,** an AChE and MAO-B dual inhibitor, was synthesised based on benzo[d]isothiazol-3(2*H*)-one[99] using the linkage approach. It showed potent AChE inhibitory activity (IC_{50} = 0.29 μM), but weak MAO-B inhibitory potency with an IC_{50} value of 20.1 μM. This potent AChE inhibition could be attributed to the compound's ability to fully occupy the entire active pocket of AChE (PDB: 1EVE), while the benzo[d]isothiazol-3-one scaffold and the benzylamine moiety generated π–π interactions with Phe331, Phe288 and Tyr130, respectively. In addition, the *S* atom established a hydrogen bond with Tyr121 in the PAS. Compared with **49**, using the fusion approach, the inhibitor **50** based on isobenzofuran-1(3*H*)-one exhibited more potent and balanced inhibitory activity against AChE and MAO-B (IC_{50} = 0.041 and 0.30 μM, respectively)[100]. It was also characterised for Cu^{2+} chelation and favourable drug-like properties. Molecular docking studies indicated that the phthalide group interacted with Tyr334 through π–π interaction, while the butyl moiety established alkyl interactions with Trp279 and Phe290 of AChE (PDB: 1EVE), respectively. Furthermore, **50** exhibited various π–π interactions and π-cation bonds with Phe330, Trp84, and Glu199 of AChE. The benzyl ether group was located in the MAO-B (PDB: 2V60) entrance cavity and formed several interactions (hydrogen bonds, π-sigma and π–π interactions) with key amino acids such as Ile199, Cys172, and Tyr326.

While most potent MAO-B inhibitors are characterised by small molecular size, an indole-based molecule of large size synthesised using the linkage approach, compound **51**, displayed potent and balanced AChE and MAO-B inhibitory activities with IC_{50} values of 0.042 and 0.33 μM, respectively[101]. These effects were attributed to its interactions with Trp86, Tyr124, Trp286, Tyr341, and Phe338 of AChE (PDB: 4EY7) through π–π interactions, as well as interactions with Gly120 and Tyr133 through hydrogen bonds. Additionally, two balanced dual inhibitors **52** and **53** (IC_{50} = 3.70 and 2.41 μM for AChE, respectively; 2.62 and 1.84 μM for MAO-B, respectively) were synthesised using the fusion approach to fuse the carbamate moiety into the indole core[102]. As expected, the carbamate moieties established π-H interactions with CAS Trp84 of AChE (PDB: 1EVE), which is an important interaction for AChE inhibition. The indole cores interacted with Trp334 and Phe330 through π–π interactions. On the other hand, **52** and **53** entered the substrate cavity of MAO-B (PDB: 2V5Z) and generated the π-H interactions with the FAD. These interactions played a crucial role in supporting the moderate MAO-B inhibitory activities observed for these two compounds.

To improve the brain permeability, the fusion approach was used to synthesise compound **55**[103] by replacing the imidazole ring of the lead **54** (IC_{50} = 0.324 and 1.427 μM, respectively) with the benzimidazole ring. Although the MAO-B inhibitory potency slightly decreased (IC_{50} = 2.117 μM), the AChE inhibitory activity significantly increased with an IC_{50} value of 0.032 μM, and the BBB permeability improved. Furthermore, **55** demonstrated the ability to reverse cognitive impairment induced by scopolamine in mice, and showed good oral bioavailability (F = 45.55%), suggesting its potential for AD therapy. Using the fusion approach, benzimidazole-based molecule **56** was obtained, exhibiting more potent and balanced dual inhibition against the two enzymes (IC_{50} = 0.024 and 0.041 μM, respectively)[104]. Aβ_{42} ligand investigation revealed that dual inhibitor **56** showed higher anti-Aβ_{42} aggregation than curcumin and similar activity to that of donepezil. Docking studies showed that the benzimidazole and the phenyl moieties generated π–π interactions with AChE (PDB: 4EY7) Trp286 and Tyr341, respectively. Besides, the quaternary amine established a hydrogen bond with Glu202. Regarding MAO-B (PDB: 2V5Z), the benzimidazole core generated π–π interaction with Trp119, and the carbonyl group formed a hydrogen bond with Tyr345.

Two indazole scaffold-based candidates **57** and **58** were created using the linkage approach, but they exhibited unbalanced dual inhibitory activities. Although they showed no AChE inhibition (21.6%, and 17.9% at 100 μM), exhibited notably MAO-B inhibitory activity (IC_{50} = 0.586, 0.386 nM respectively)[105]. This result suggested that the presence of AChE inhibitory moieties was indispensable for the AChE and MAO-B dual inhibitors. The docking study of potent and balanced dual inhibitors **59** and **60** (IC_{50} = 23.4, and 27.8 nM for AChE, respectively; 40.3 and 56.7 nM

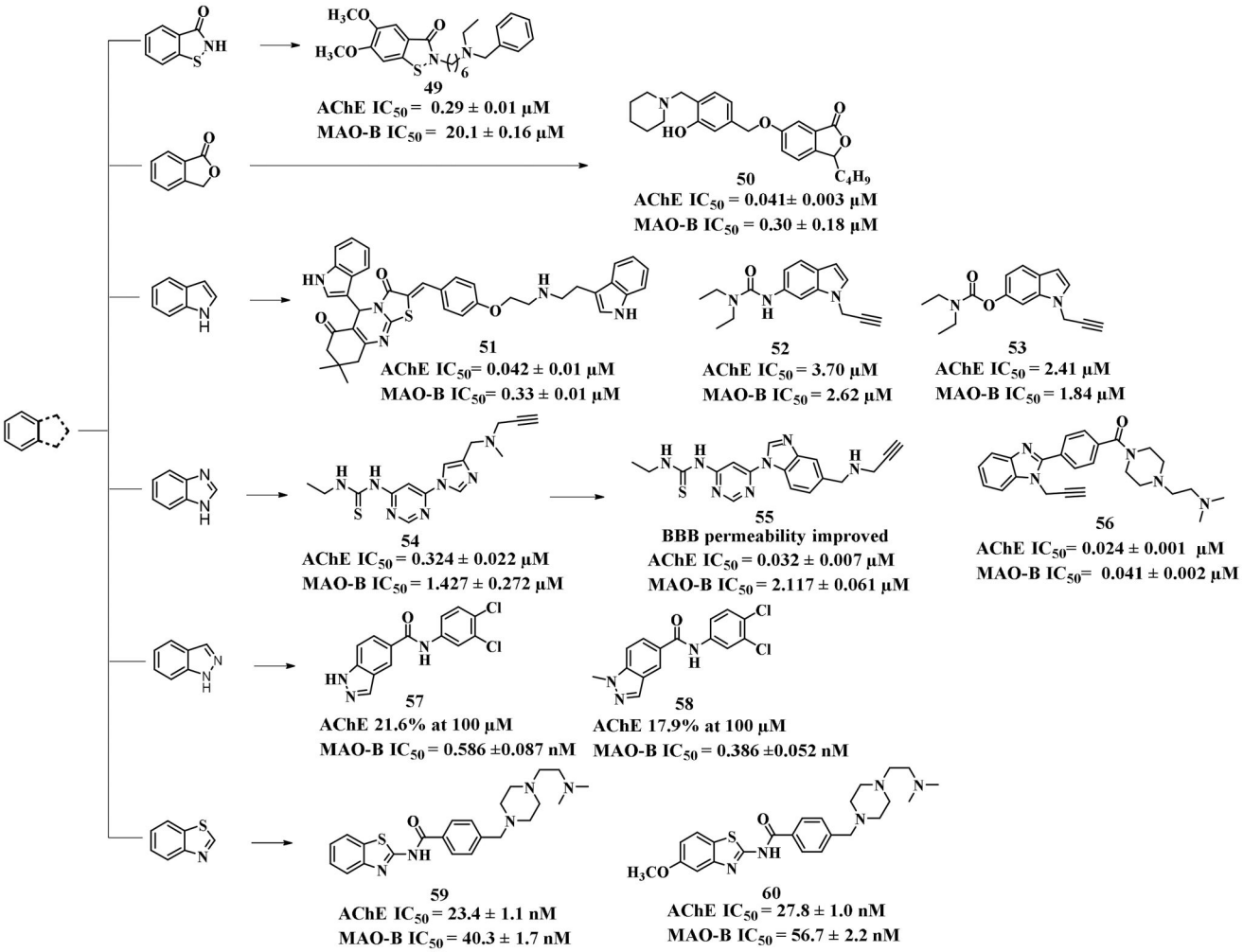

Figure 13. Structures of benzo five-membered ring-based inhibitors.

for MAO-B, respectively)[106] obtained by using the fusion approach, further supported this observation. Both compounds were derived from a benzothiazole scaffold. In the AChE (PDB: 4EY7) docking study, the benzothiazole moiety of dual inhibitor **59** established π–π interaction with Trp286, and its carbonyl moiety formed a hydrogen bond with Phe295 in PAS. The *N* atoms of piperazine bound to Trp86 and Try337 by cation-π interactions, and a salt bridge was established with Asp74. Additionally, the *N* atom of dimethylaminoethyl moiety generated a hydrogen bond with Ser125. In the MAO-B (PDB: 2V5Z) docking study, the benzothiazole ring formed an aromatic-hydrogen bond with Pro102. The terminal *N* atom of the dimethylaminoethyl side chain and the *N* atom in the 1st position of the piperazine established cation–π interactions with Try435 and Tyr398, respectively. In addition, the piperazine ring formed a hydrogen bond with the carbonyl adjacent to the N5 of FAD.

Imine and hydrazone-based inhibitors

The C = N group has been widely reported as effective regulator of the interaction between inhibitors and enzyme, thus making imine and hydrazone derivatives potent MAO-B inhibitors in the past[107]. Moreover, the imine nitrogen of the hydrazine could form a hydrogen bond with Tyr407[108]. Therefore, the C = N group has been widely investigated as an effective linker in seeking for potent AChE and MAO-B dual inhibitors (Figure 14).

Several imine-based anti-AD compounds have been synthesised using the linkage approach, and evaluated by researchers[105,109,110]. However, these compounds such as compounds **61** and **62**, showed unbalanced dual-target inhibitory potency, with no AChE inhibition, but potent MAO-B inhibitory abilities (IC_{50} values of 0.612 and 0.049 μM, respectively). Compared to **61** and **62**, compound **63** displayed potent AChE inhibitory activity (IC_{50} = 0.057 μM), but remained an unbalanced MAO-B inhibitor (52.28% at 1 mM). Interestingly, a series of potent and balanced dual inhibitors (**64–67**)[111–113] were obtained using the linkage approach when the hydrazone was designed as a linker to the substitute imine group.

The piperonylic acid derived hydrazones **64** (IC_{50} = 0.052 μM for AChE, and 0.89 μM for MAO-B) and **65** (IC_{50} = 0.85 μM for AChE and 0.034 μM for MAO-B) displayed balanced inhibitory activities against target enzymes. But **65** demonstrated more potent MAO-B inhibitory potency, suggesting that the propargyl substitution could improve the MAO-B inhibitory potency. In the AChE (PDB: 4EY7) binding mode, **64** formed two hydrogen bonds with Asp74 and Phe295, and **65** formed four hydrogen bonds with Phe295, Gly122, Gly121, and Ala204. Additionally, hydrophobic interactions established between both compounds and Val294, Phe338, Tyr337, and Trp28 were observed. Regarding MAO-B

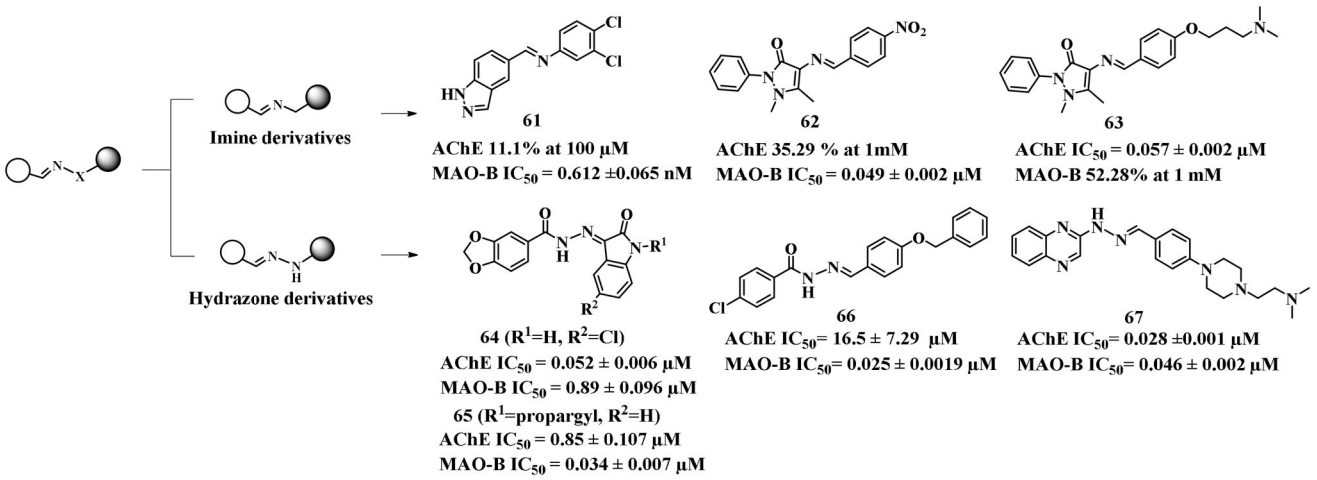

Figure 14. Structures of imine and hydrazone-based inhibitors.

(PDB: 2V5Z), the isatin moieties of both compounds were oriented towards FAD, and a hydrogen bond was established between **64** and Tyr435, while four hydrogen bonds were observed between **65** and Ile199, Tyr326, Gln206, and Ile198.

The aromatic aldehyde hydrazone derivative **66**[112] was created by using the linkage approach. It exhibited weak AChE inhibition (IC_{50} = 16.5 μM), but showed excellent MAO-B inhibitory potency with an IC_{50} value of 0.025 μM, possibly due to the absence of AChE inhibitory pharmacophore. In the light of this, the potent and balanced quinoxaline scaffold-based dual inhibitor **67** was developed by using the linkage approach to fuse the AChE CAS inhibitory pharmacophore[103]. This lead compound showed potent and balanced AChE and MAO-B inhibitory activity (IC_{50} = 0.028 and 0.046 μM, respectively). In the AChE (PDB: 4EY7) docking study, π–π interactions were established between the quinoxaline and Trp286, as well as the phenyl ring and Phe338, and Tyr341. Two crucial hydrogen bonds were established between the hydrazone moiety with Arg296 and Phe295, respectively. In addition, the *N* atom of the dimethylaminoalkyl fragment formed a salt bridge with Glu202. In the docking study of MAO-B (PDB: 2V5Z), the quinoxaline core and phenyl ring bound to Tyr435 and Tyr326 through π–π interactions, respectively. The hydrazine and dimethylaminoalkyl moieties formed hydrogen bonds with Glu206 and Pro102, respectively.

Other scaffold-based inhibitors

In addition to the AChE and MAO-B candidates mentioned above, extensive research has been conducted on other scaffold-based dual inhibitors (Figure 15). Compound **68,** 3,4-dihydropyrimidin-2(1*H*)-one-based dual inhibitor[114], showed moderate AChE inhibitory potency and potent MAO-B inhibitory activity with IC_{50} values of 2.86 and 0.34 μM, respectively. Another potent and balanced dual inhibitor, pyridoxine scaffold-based compound **69** (IC_{50} = 0.081 and 0.039 μM, respectively) was synthesised using the linkage approach[115]. A docking study showed that it bound to Tyr435 and Tyr398 of AChE (PDB: 4EY7) through π–π interactions, and embedded in the entrance cavity of MAO-B (PDB: 2BYB) which was formed by Tyr69, Ile199, Leu167, Gln206, Ile316, and Leu171. In addition, notable π–π interactions were observed with Tyr435 and Tyr398 in the substrate cavity of MAO-B.

Youdim[50] designed and synthesised the inhibitor **70** using the fusion approach, which served as the prodrug for compound **71**. Compound **70** showed potent AChE inhibitory activity with an IC_{50} value of 0.52 μM, but exhibited limited MAO-B inhibitory potency (IC_{50} = 7.90 μM) and metal affinity (Fe, Cu, and Zn). Interestingly, upon metabolism by AChE, it released **71** to restore the abilities of metal ions chelation and MAO-B inhibitory activity (IC_{50} = 0.057 μM), suggesting that **70** hold promise as a multi-target lead for AD therapy. Compound **72**, synthesised using the linkage approach, was a dual inhibitor based on 1(2*H*)-phthalazinone scaffold[116]. Although various interactions such as hydrogen bond and π–π interactions have been established (AChE, PDB: 1EVE), it displayed only moderate AChE inhibition (IC_{50} = 8.2 μM). However, it exhibited potent MAO-B inhibitory activity with an IC_{50} value of 0.7 μM. In the MAO-B (PDB: 2V60) docking study, the phthalazinone core of **72** formed hydrogen bonds with crucial residues Cys172 and Tyr407. Similarly, compounds **73**, **74,** and **75** were obtained using the linkage or fusion approaches. They displayed moderate AChE inhibition (IC_{50} = 2.9, 0.442, and 7.31 μM, respectively), but weak MAO-B inhibition (IC_{50} = 16.6, 6.43, and 26.1 μM, respectively)[117–119], suggesting that a rigid scaffold is necessary for potent MAO-B inhibitors.

Fluoxetine and sertraline, used as antidepressant drugs in clinical practice, have recently been explored for the design of anti-AD drugs. Nadeem et al.[120] developed a series of potent and balanced AChE and MAO-B dual inhibitors by using the linkage approach to fuse the structural features from fluoxetine and sertraline into the tacrine, donepezil, and certain antidiabetic drugs (pioglitazone, ciglitazone, rosiglitazone, and troglitazone). Among them, **76–80** exhibited the best dual inhibitory activities (IC_{50} = 0.024, 0.010, 0.035, 0.015, and 0.008 μM for AChE, respectively; IC_{50} = 0.011, 0.015, 0.180, 0.157, and 0.031 μM for MAO-B, respectively), and showed good safety profiles (2000 mg·kg^{-1}). Molecular docking studies revealed that these compounds could interact with residues of AChE (PDB: 2CKM) including Trp84, Phe330, Trp279, and Tyr70 through π–π interactions. Besides, hydrogen bonds were observed with Tyr121 and Tyr334. In the case of MAO-B (PDB: 2V5Z), these compounds established hydrogen bonds with Tyr188, Tyr326, and Trp388, and π–π interactions with Tyr398 and Tyr435.

The diclofenac derivative **81** displayed moderate AChE inhibition (IC_{50} = 2.58 μM) but weak MAO-B inhibition (IC_{50} = 13.07 μM). In order to discover potent and balanced AChE and MAO-B dual inhibitors, Javed's group[121] synthesised several diclofenac derivatives based on the lead **81** by using the linkage or fusion approaches. Among them, **82**, **83,** and **84** demonstrated potent and balanced AChE and MAO-B inhibitory activities. In

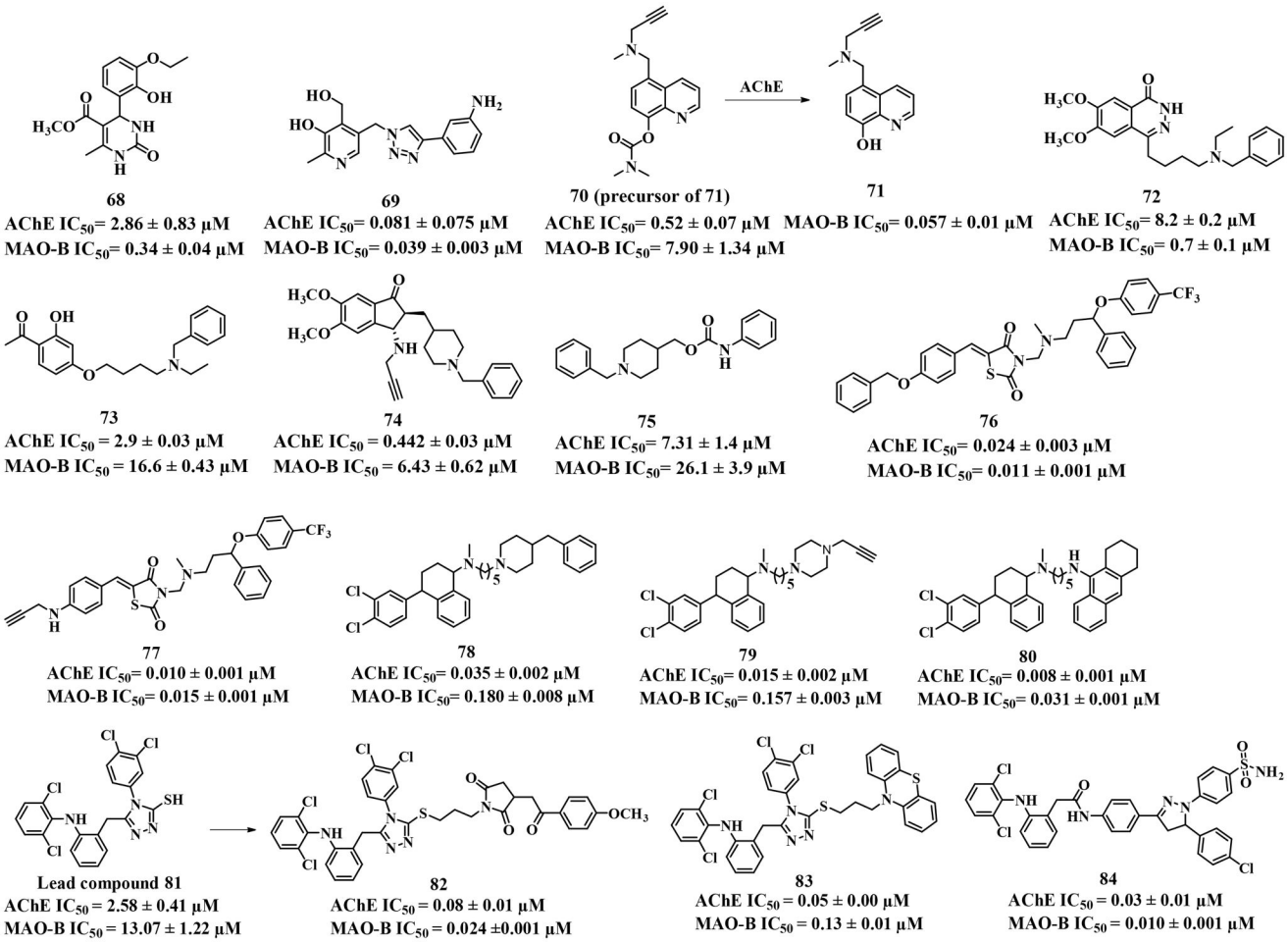

Figure 15. Structures of other scaffold-based inhibitors.

particular, **84** exhibited the ability to cross the BBB and demonstrated non-neurotoxicity at the dose of 2000 mg kg^{-1} *in vivo*. Docking studies demonstrated the formation of π–π, hydrogen bond, and π-*S* interactions between **84** and Trp84, Phe330, Phe331, Tyr121, Trp279, and Tyr334 of AChE (PDB: 1EVE). On the other hand, six hydrogen bonds were observed between **84** and Arg42, Cys197, Ile199, Gln206, Tyr326, and Trp388 of MAO-B (PDB: 2V5Z). These interactions provided an explanation for its functional profiles.

Conclusion and prospect

In spite of AChE has been the most successful target in development of anti-AD drugs, AChEIs approved by FDA have been only employed for symptomatic treatment of AD. MAO-B has emerged as another promising target against AD due to the discovery of its overexpression in AD patients' brain and the establishment of an oxidative stress state. Therefore, we have conducted a comprehensive review of the dual inhibitors targeting both AChE and MAO-B published in recent years.

The methods for implementing MTDLs strategy and the primary characteristics of AChE and MAO-B active pockets were summarised in this review. Based on this, dual inhibitors targeting both AChE and MAO-B, including chalcone, couumarin, chromone, benzo five-membered ring, imine, and hydrazone scaffolds, were systematically classified according to their structural characteristics. Additionally, an in-depth analysis of their design strategies, docking studies, and SARs was conducted. Phe295, Phe288, and Tyr121 of AChE could form hydrogen bonds with ligands, and Trp279, Trp286, Phe330, Phe334, Phe338, and Tyr341 generated π–π interactions. Moreover, Tyr72 and Tyr334 established hydrogen bonds and π–π interactions. Similarly, Cys172, Ile198, Ile199, Gln206, Tyr188, Arg42, and Pro102 of MAO-B could form hydrogen bonds with ligands, Tyr326, Tyr398, and Tyr435 established hydrogen bonds and π–π interactions. These above-mentioned residues played a crucial role in determining the AChE and MAO-B inhibitory activities of ligands, providing the useful clues for designing reasonable dual inhibitors of AChE and MAO-B by predicting whether ligands could generate interactions with these crucial residues.

However, great challenges still exist to develop balanced and potent dual inhibitors targeting both AChE and MAO-B due to the inherent structural limitations of both enzymes themselves. The CAS site for AChE is located at the bottom of a deep and narrow gorge (about 20 Å long and as narrow as 4.5 Å). While the active sites of MAO-B is composed of the "entrance cavity" (about 290 $Å^3$) and a larger hydrophobic substrate cavity (420 $Å^3$). This meant that both enzymes often lack the ability to share the same pharmacophores, making the discovery of potent and balanced dual inhibitors of AChE and MAO-B an extremely difficult process. With the advancement of artificial intelligence, CADD strategies have played an important role in new drug discovery, offering an effective approach to solve this challenge. The high-throughput screening, energy calculation, affinity prediction based on this technique can significantly improve the efficiency in designing dual inhibitors of AChE and MAO-B, avoiding the arduous process

of blind phenotype-based screening, and creating the well-balanced and potent candidates that cross the BBB with high bioavailability and low toxic side effects.

Encouragingly, lecanemab, the second Aβ-targeting drug after aducanumab, has been fully approved by the FDA for the treatment of AD this year. This approval not only provides solid evidence for the Aβ hypothesis of AD, but also represents a significant milestone in AD therapy, bringing new hope for AD patients. In addition, due to the complex nature of AD, various therapies are undergoing clinical trials, such as anti-tau, synaptic plasticity/neuroprotection, and anti-inflammation therapies. Furthermore, recent studies have identified new opportunities and possible targets for AD therapy such as β2-microglobulin, microRNA-132, and Bacillus Calmette-Guérin. With the continuous advancement of research, the complex nature of AD will gradually be understood, leading to the discovery of more effective drugs. The treatment of AD will present diverse prospects and the combination of multiple approaches may bring more clinical benefits to AD patients.

Authors contributions

Writing-original draft preparation, Dajiang Zou; writing-review and editing, Dajiang Zou, Renzheng Liu, Yangjing Lv, Jianan Guo, Changjun Zhang; supervision, Yuanyuan Xie. All authors have read and agreed to the published version of the manuscript.

Disclosure statement

No potential conflict of interest was reported by the author(s).

Funding

This project was supported by the Zhejiang Key R&D Program (No. 2021C03085); National Key R&D Program of China (2021YFC2100800); National Natural Science Foundation of China, NSFC (Grant No. 21978273 and 22378360); China Postdoctoral Science Foundation, CPSF (No. 2021M702897).

ORCID

Changjun Zhang http://orcid.org/0000-0002-7088-146X
Yuanyuan Xie http://orcid.org/0000-0001-8482-9948

References

1. Gustavsson A, Norton N, Fast T, Froelich L, Georges J, Holzapfel D, Kirabali T, Krolak-Salmon P, Rossini PM, Ferretti MT, et al. Global estimates on the number of persons across the Alzheimer's disease continuum. Alzheimers Dement. 2022;19:658–670.
2. Nichols E, Szoeke CEI, Vollset SE, Abbasi N, Abd-Allah F, Abdela J, Aichour MTE, Akinyemi RO, Alahdab F, Asgedom SW, et al. Global, regional, and national burden of Alzheimer's disease and other dementias, 1990–2016: A systematic analysis for the global burden of disease study 2016. Lancet Neurol. 2019;18(1):88–106.
3. Vos T, Lim SS, Abbafati C, Abbas KM, Abbasi M, Abbasifard M, Abbasi-Kangevari M, Abbastabar H, Abd-Allah F, Abdelalim A, et al. Global burden of 369 diseases and injuries in 204 countries and territories, 1990–2019: A systematic analysis for the global burden of disease study 2019. Lancet. 2020;396(10258):1204–1222.
4. Yang AC, Vest RT, Kern F, Lee DP, Agam M, Maat CA, Losada PM, Chen MB, Schaum N, Khoury N, et al. A human brain vascular atlas reveals diverse mediators of Alzheimer's risk. Nature. 2022;603(7903):885–892.
5. Fang X, Zhang J, Roman RJ, Fan F. From 1901 to 2022, how far are we from truly understanding the pathogenesis of age-related dementia? Geroscience. 2022;44(3):1879–1883.
6. Zhang P, Xu S, Zhu Z, Xu J. Multi-target design strategies for the improved treatment of Alzheimer's disease. Eur J Med Chem. 2019;176:228–247.
7. Sharma K. Cholinesterase inhibitors as Alzheimer's therapeutics. Mol Med Rep. 2019;20(2):1479–1487.
8. Castro A, Martinez A. Targeting β-amyloid pathogenesis through acetylcholinesterase inhibitors. Curr Pharm Des. 2006;12(33):4377–4387.
9. Tripathi AC, Upadhyay S, Paliwal S, Saraf SK. Privileged scaffolds as MAO inhibitors: retrospect and prospects. Eur J Med Chem. 2018;145:445–497.
10. Mpitimpiti AN, Petzer JP, Petzer A, Jordaan JHL, Lourens ACU. Synthesis and evaluation of chromone derivatives as inhibitors of monoamine oxidase. Mol Divers. 2019;23(4):897–913.
11. Santin Y, Resta J, Parini A, Mialet-Perez J. Monoamine oxidases in age-associated diseases: new perspectives for old enzymes. Ageing Res Rev. 2021;66:101256.
12. Ramsay RR. Molecular aspects of monoamine oxidase B. Prog Neuropsychopharmacol Biol Psychiatry. 2016;69:81–89.
13. Inaba-Hasegawa K, Akao Y, Maruyama W, Naoi M. Rasagiline and selegiline, inhibitors of type B monoamine oxidase, induce type A monoamine oxidase in human SH-SY5Y cells. J Neural Transm. 2013;120(3):435–444.
14. Finberg JPM. Update on the pharmacology of selective inhibitors of MAO-A and MAO-B: focus on modulation of CNS monoamine neurotransmitter release. Pharmacol Ther. 2014;143(2):133–152.
15. Srivastava S, Ahmad R, Khare SK. Alzheimer's disease and its treatment by different approaches: a review. Eur J Med Chem. 2021;216:113320.
16. Knez D, Sova M, Kosak U, Gobec S. Dual inhibitors of cholinesterases and monoamine oxidases for Alzheimer's disease. Future Med Chem. 2017;9(8):811–832.
17. Cavalli A, Bolognesi ML, Minarini A, Rosini M, Tumiatti V, Recanatini M, Melchiorre C. Multi-target-directed ligands to combat neurodegenerative diseases. J Med Chem. 2008;51(3):347–372.
18. Benek O, Korabecny J, Soukup O. A perspective on multitarget drugs for Alzheimer's disease. Trends Pharmacol Sci. 2020;41(7):434–445.
19. Mesiti F, Chavarria D, Gaspar A, Alcaro S, Borges F. The chemistry toolbox of multitarget-directed ligands for Alzheimer's disease. Eur J Med Chem. 2019;181:111572.
20. Nozal V, García-Rubia A, Cuevas EP, Pérez C, Tosat-Bitrián C, Bartolomé F, Carro E, Ramírez D, Palomo V, Martínez A. From kinase inhibitors to multitarget ligands as powerful drug leads for Alzheimer's disease using protein-templated synthesis. Angew Chem Int Ed Engl. 2021;60(35):19344–19354.
21. Savelieff MG, Nam G, Kang J, Lee HJ, Lee M, Lim MH. Development of multifunctional molecules as potential

therapeutic candidates for Alzheimer's disease, Parkinson's disease, and amyotrophic lateral sclerosis in the last decade. Chem Rev. 2019;119(2):1221–1322.
22. Tumiatti V, Minarini A, Bolognesi ML, Milelli A, Rosini M, Melchiorre C. Tacrine derivatives and Alzheimer's disease. Curr Med Chem. 2010;17(17):1825–1838.
23. Li SY, Jiang N, Xie SS, Wang KDG, Wang XB, Kong LY. Design, synthesis and evaluation of novel tacrine-rhein hybrids as multifunctional agents for the treatment of Alzheimer's disease. Org Biomol Chem. 2014;12(5):801–814.
24. Faller P. Copper and zinc binding to amyloid-β: coordination, dynamics, aggregation, reactivity and metal-ion transfer. Chembiochem. 2009;10(18):2837–2845.
25. Zhang Y, Chen LY, Yin WX, Yin J, Zhang SB, Liu CL. The chelation targeting metal-Aβ_{40} aggregates may lead to formation of Aβ_{40} oligomers. Dalton Trans. 2011;40(18):4830–4833.
26. Bolognin S, Drago D, Messori L, Zatta P. Chelation therapy for neurodegenerative diseases. Med Res Rev. 2009;29(4):547–570.
27. Rodríguez-Rodríguez C, Sánchez de Groot N, Rimola A, Alvarez-Larena A, Lloveras V, Vidal-Gancedo J, Ventura S, Vendrell J, Sodupe M, González-Duarte P. Design, selection, and characterization of thioflavin-based intercalation compounds with metal chelating properties for application in Alzheimer's disease. J Am Chem Soc. 2009;131(4):1436–1451.
28. Takao K, Kubota Y, Kamauchi H, Sugita Y. Synthesis and biological evaluation of pyrano [4,3-b][1] benzopyranone derivatives as monoamine oxidase and cholinesterase inhibitors. Bioorg Chem. 2019;83:432–437.
29. Seenuvasan M, Vinodhini G, Malar CG, Balaji N, Kumar KS. Magnetic nanoparticles: a versatile carrier for enzymes in bio-processing sectors. IET Nanobiotechnol. 2018;12(5):535–548.
30. Zhang F, Li SH, Liu C, Fang K, Jiang YM, Zhang JY, Lan J, Zhu L, Pang HQ, Wang G. Rapid screening for acetylcholinesterase inhibitors in *Selaginella doederleinii* hieron by using functionalized magnetic Fe_3O_4 nanoparticles. Talanta. 2022;243:123284.
31. Li CH, Wang WF, Stanislas N, Yang JL. Facile preparation of fluorescent water-soluble non-conjugated polymer dots and fabricating an acetylcholinesterase biosensor. RSC Adv. 2022;12(13):7911–7921.
32. Liao CZ, Sitzmann M, Pugliese A, Nicklaus MC. Software and resources for computational medicinal chemistry. Future Med Chem. 2011;3(8):1057–1085.
33. Zhou P, Hua F. Exploration of acetylcholinesterase inhibitors from flavonoids and flavonoid glycosides. Neurochem J. 2020;14(3):251–256.
34. Gidaro MC, Astorino C, Petzer A, Carradori S, Alcaro F, Costa G, Artese A, Rafele G, Russo FM, Petzer JP, et al. Kaempferol as selective human MAO-A inhibitor: analytical detection in calabrian red wines, biological and molecular modeling studies. J Agric Food Chem. 2016;64(6):1394–1400.
35. Gogineni V, Nael MA, Chaurasiya ND, Elokely KM, McCurdy CR, Rimoldi JM, Cutler SJ, Tekwani BL, Leon F. Computationally assisted lead optimization of novel potent and selective MAO-B inhibitors. Biomedicines. 2021;9(10):1304.
36. Wang D, Chen NH, Taranto AG, Jin YT, Wen CC, Kong DX. Accelerating the identification of subtype selective inhibitors via three-dimensional biologically relevant spectrum (BRS-3D): The monoamine oxidase subtypes as a case study. Bioorg Chem. 2021;106:104503.
37. Kessel D. Photodynamic therapy: a brief history. J Clin Med. 2019;8(10):1581.
38. Paolino M, Rullo M, Maramai S, de Candia M, Pisani L, Catto M, Mugnaini C, Brizzi A, Cappelli A, Olivucci M, et al. Design, synthesis and biological evaluation of light-driven on-off multitarget AChE and MAO-B inhibitors. RSC Med Chem. 2022;13(7):873–883.
39. Farina R, Pisani L, Catto M, Nicolotti O, Gadaleta D, Denora N, Soto-Otero R, Mendez-Alvarez E, Passos CS, Muncipinto G, et al. Structure-based design and optimization of multitarget-directed 2*H*-chromen-2-one derivatives as potent inhibitors of monoamine oxidase B and cholinesterases. J Med Chem. 2015;58(14):5561–5578.
40. Greenblatt HM, Dvir H, Silman I, Sussman JL. Acetylcholinesterase – a multifaceted target for structure-based drug design of anticholinesterase agents for the treatment of Alzheimer's disease. J Mol Neurosci. 2003;20(3):369–383.
41. Agatonovic-Kustrin S, Kettle C, Morton DW. A molecular approach in drug development for Alzheimer's disease. Biomed Pharmacother. 2018;106:553–565.
42. Milczek EM, Binda C, Rovida S, Mattevi A, Edmondson DE. The 'gating' residues ile199 and tyr326 in human monoamine oxidase B function in substrate and inhibitor recognition. Febs J. 2011;278(24):4860–4869.
43. Hubalek F, Binda C, Li M, Herzig Y, Sterling J, Youdim MBH, Mattevi A, Edmondson DE. Inactivation of purified human recombinant monoamine oxidases A and B by rasagiline and its analogues. J Med Chem. 2004;47(7):1760–1766.
44. Zhang C, Lv Y, Bai R, Xie Y. Structural exploration of multifunctional monoamine oxidase B inhibitors as potential drug candidates against Alzheimer's disease. Bioorg Chem. 2021;114:105070.
45. De Colibus L, Li M, Binda C, Lustig A, Edmondson DE, Mattevi A. Three-dimensional structure of human monoamine oxidase A (MAO-A): relation to the structures of rat MAO-A and human MAO-B. Proc Natl Acad Sci U S A. 2005;102(36):12684–12689.
46. Li M, Binda C, Mattevi A, Edmondson DE. Functional role of the "aromatic cage" in human monoamine oxidase B: structures and catalytic properties of tyr435 mutant proteins. Biochemistry. 2006;45(15):4775–4784.
47. Więckowska A, Szałaj N, Góral I, Bucki A, Latacz G, Kiec-Kononowicz K, Bautista-Aguilera ÒM, Romero A, Ramos E, Egea J, et al. In vitro and in silico ADME-Tox profiling and safety significance of multifunctional monoamine oxidase inhibitors targeting neurodegenerative diseases. ACS Chem Neurosci. 2020;11(22):3793–3801.
48. del Pino J, Marco-Contelles J, Lopez-Munoz F, Romero A, Ramos E. Neuroinflammation signaling modulated by ASS234, a multitarget small molecule for Alzheimer's disease therapy. ACS Chem Neurosci. 2018;9(12):2880–2885.
49. Marco-Contelles J, Unzeta M, Bolea I, Esteban G, Ramsay RR, Romero A, Martínez-Murillo R, Carreiras MC, Ismaili L. ASS234, as a new multi-target directed propargylamine for Alzheimer's disease therapy. Front Neurosci. 2016;10:294.
50. Youdim MBH. Site-activated multi target iron chelators with acetylcholinesterase (AChE) and monoamine oxidase (MAO) inhibitory activities for Alzheimer's disease therapy. J Neural Transm. 2022;129(5-6):715–721.

51. Weinstock M, Kirschbaum-Slager N, Lazarovici P, Bejar C, Youdim MBH, Shoham S. Neuroprotective effects of novel cholinesterase inhibitors derived from rasagiline as potential anti-Alzheimer drugs. Ann N Y Acad Sci. 2001;939:148–161.
52. Weinstock M, Gorodetsky E, Wang RH, Gross A, Weinreb O, Youdim MBH. Limited potentiation of blood pressure response to oral tyramine by brain-selective monoamine oxidase A-B inhibitor, TV-3326 in conscious rabbits. Neuropharmacology. 2002;43(6):999–1005.
53. Xu Y-X, Wang H, Li X-K, Dong S-N, Liu W-W, Gong Q, Wang T-D-Y, Tang Y, Zhu J, Li J, et al. Discovery of novel propargylamine-modified 4-aminoalkyl imidazole substituted pyrimidinylthiourea derivatives as multifunctional agents for the treatment of Alzheimer's disease. Eur J Med Chem. 2018;143:33–47.
54. Zhuang C, Zhang W, Sheng C, Zhang W, Xing C, Miao Z. Chalcone: A privileged structure in medicinal chemistry. Chem Rev. 2017;117(12):7762–7810.
55. Zhou B, Xing C. Diverse molecular targets for chalcones with varied bioactivities. Med Chem. 2015;5(8):388–404.
56. Oh JM, Kang M-G, Hong A, Park J-E, Kim SH, Lee JP, Baek SC, Park D, Nam S-J, Cho M-L, et al. Potent and selective inhibition of human monoamine oxidase-B by 4-dimethylaminochalcone and selected chalcone derivatives. Int J Biol Macromol. 2019;137:426–432.
57. Lakshminarayanan B, Baek SC, Lee JP, Kannappan N, Mangiatordi GF, Nicolotti O, Subburaju T, Kim H, Mathew B. Ethoxylated head of chalcones as a new class of multi-targeted MAO inhibitors. Chemistryselect. 2019;4(21):6614–6619.
58. Sasidharan R, Eom BH, Heo JH, Park JE, Abdelgawad MA, Musa A, Gambacorta N, Nicolotti O, Manju SL, Mathew B, et al. Morpholine-based chalcones as dual-acting monoamine oxidase-B and acetylcholinesterase inhibitors: synthesis and biochemical investigations. J Enzyme Inhib Med Chem. 2021;36(1):188–197.
59. Mathew B, Oh JM, Baty RS, Batiha GE-S, Parambi DGT, Gambacorta N, Nicolotti O, Kim H. Piperazine-substituted chalcones: a new class of MAO-B, AChE, and BACE-1 inhibitors for the treatment of neurological disorders. Environ Sci Pollut Res Int. 2021;28(29):38855–38866.
60. Yamali C, Engin FS, Bilginer S, Tugrak M, Ozmen Ozgun D, Ozli G, Levent S, Saglik BN, Ozkay Y, Gul HI. Phenothiazine-based chalcones as potential dual-target inhibitors toward cholinesterases (AChE, BuChE) and monoamine oxidases (MAO-A, MAO-B). J Heterocycl Chem. 2021;58(1):161–171.
61. Jeong GS, Kaipakasseri S, Lee SR, Marraiki N, Batiha GE-S, Dev S, Palakkathondi A, Kavully FS, Gambacorta N, Nicolotti O, et al. Selected 1,3-benzodioxine-containing chalcones as multipotent oxidase and acetylcholinesterase inhibitors. ChemMedChem. 2020;15(23):2257–2263.
62. Sang Z, Song Q, Cao Z, Deng Y, Zhang L. Design, synthesis, and evaluation of chalcone-vitamin E-donepezil hybrids as multi-target-directed ligands for the treatment of Alzheimer's disease. J Enzyme Inhib Med Chem. 2022;37(1):69–85.
63. Sang Z, Song Q, Cao Z, Deng Y, Tan Z, Zhang L. Design, synthesis and evaluation of novel dimethylamino chalcone-O-alkylamines derivatives as potential multifunctional agents against Alzheimer's disease. Eur J Med Chem. 2021;216:113310.
64. Bai P, Wang K, Zhang P, Shi J, Cheng X, Zhang Q, Zheng C, Cheng Y, Yang J, Lu X, et al. Development of chalcone-O-alkylamine derivatives as multifunctional agents against Alzheimer's disease. Eur J Med Chem. 2019;183:111737.
65. Sang Z, Wang K, Shi J, Liu W, Tan Z. Design, synthesis, in-silico and biological evaluation of novel chalcone-*O*-carbamate derivatives as multifunctional agents for the treatment of Alzheimer's disease. Eur J Med Chem. 2019;178:726–739.
66. Park DH, Venkatesan J, Kim SK, Ramkumar V, Parthiban P. Antioxidant properties of Mannich bases. Bioorg Med Chem Lett. 2012;22(20):6362–6367.
67. Roman G. Mannich bases in medicinal chemistry and drug design. Eur J Med Chem. 2015;89:743–816.
68. Buyukkidan N, Ozer S. Synthesis and characterization of Ni(ii) and Cu(ii) complexes derived from novel phenolic Mannich bases. Turk J Chem. 2013;37(1):101–110.
69. Bui TH, Le TT, Vu TT, Hoang XT, Luu VC, Vu DH, Tran KV. Design, synthesis and in vitro cytotoxic activity evaluation of new Mannich bases. B Korean Chem Soc. 2012;33(5):1586–1592.
70. Tian C, Qiang X, Song Q, Cao Z, Ye C, He Y, Deng Y, Zhang L. Flurbiprofen-chalcone hybrid Mannich base derivatives as balanced multifunctional agents against Alzheimer's disease: Design, synthesis and biological evaluation. Bioorg Chem. 2020;94:103477.
71. Zhang X, Song Q, Cao Z, Li Y, Tian C, Yang Z, Zhang H, Deng Y. Design, synthesis and evaluation of chalcone Mannich base derivatives as multifunctional agents for the potential treatment of Alzheimer's disease. Bioorg Chem. 2019;87:395–408.
72. Oh JM, Rangarajan TM, Chaudhary R, Singh RP, Singh M, Singh RP, Tondo AR, Gambacorta N, Nicolotti O, Mathew B, et al. Novel class of chalcone oxime ethers as potent monoamine oxidase-B and acetylcholinesterase inhibitors. Molecules. 2020;25(10):2356.
73. Oh JM, Rangarajan TM, Chaudhary R, Gambacorta N, Nicolotti O, Kumar S, Mathew B, Kim H. Aldoxime- and hydroxy-functionalized chalcones as highly potent and selective monoamine oxidase-B inhibitors. J Mol Struct. 2022;1250:131817.
74. Kumar B, Dwivedi AR, Sarkar B, Gupta SK, Krishnamurthy S, Mantha AK, Parkash J, Kumar V. 4,6-diphenylpyrimidine derivatives as dual inhibitors of monoamine oxidase and acetylcholinesterase for the treatment of Alzheimer's disease. ACS Chem Neurosci. 2019;10(1):252–265.
75. Kumar B, Kumar V, Prashar V, Saini S, Dwivedi AR, Bajaj B, Mehta D, Parkash J, Kumar V. Dipropargyl substituted diphenylpyrimidines as dual inhibitors of monoamine oxidase and acetylcholinesterase. Eur J Med Chem. 2019;177:221–234.
76. Kurt BZ, Gazioglu I, Sonmez F, Kucukislamoglu M. Synthesis, antioxidant and anticholinesterase activities of novel coumarylthiazole derivatives. Bioorg Chem. 2015;59:80–90.
77. Xia-Hou ZR, Feng XF, Mei YF, Zhang YY, Yang T, Pan J, Yang JH, Wang YS. 5-Demethoxy-10′-ethoxyexotimarin F, a new coumarin with MAO-B inhibitory potential from Murraya exotica L. Molecules. 2022;27(15):4950.
78. Maliyakkal N, Ahmad I, Kumar S, Sudevan ST, Beeran AA, Patel H, Kim H, Mathew B. A structural approach to investigate halogen substituted MAO-B inhibitors using QSAR

modeling, molecular dynamics, and conceptual DFT analysis. J Saudi Chem Soc. 2023;27(4):101675.
79. Joubert J, Foka GB, Repsold BP, Oliver DW, Kapp E, Malan SF. Synthesis and evaluation of 7-substituted coumarin derivatives as multimodal monoamine oxidase-B and cholinesterase inhibitors for the treatment of Alzheimer's disease. Eur J Med Chem. 2017;125:853–864.
80. Bester E, Petzer A, Petzer JP. Coumarin derivatives as inhibitors of D-amino acid oxidase and monoamine oxidase. Bioorg Chem. 2022;123:105791.
81. Lan JS, Ding Y, Liu Y, Kang P, Hou JW, Zhang XY, Xie SS, Zhang T. Design, synthesis and biological evaluation of novel coumarin-N-benzyl pyridinium hybrids as multi-target agents for the treatment of Alzheimer's disease. Eur J Med Chem. 2017;139:48–59.
82. Fonseca A, Matos MJ, Reis J, Duarte Y, Gutierrez M, Santana L, Uriarte E, Borges F. Exploring coumarin potentialities: development of new enzymatic inhibitors based on the 6-methyl-3-carboxamidocoumarin scaffold. RSC Adv. 2016;6(55):49764–49768.
83. Vina D, Matos MJ, Yanez M, Santana L, Uriarte E. 3-substituted coumarins as dual inhibitors of AChE and MAO for the treatment of Alzheimer's disease. Medchemcomm. 2012;3(2):213–218.
84. Zhang Q, Hao C, Miao Y, Yun Y, Sun X, Pan Y, Sun J, Wang X. Design and synthesis of benzyl aminocoumarin and its anti-Alzheimer's activity. New J Chem. 2021;45(37):17287–17300.
85. Rehuman NA, Oh JM, Nath LR, Khames A, Abdelgawad MA, Gambacorta N, Nicolotti O, Jat RK, Kim H, Mathew B. Halogenated coumarin-chalcones as multifunctional monoamine oxidase-B and butyrylcholinesterase inhibitors. Acs Omega. 2021;6(42):28182–28193.
86. Rodriguez-Enriquez F, Vina D, Uriarte E, Laguna R, Matos MJ. 7-amidocoumarins as multitarget agents against neurodegenerative diseases: substitution pattern modulation. Chemmedchem. 2021;16(1):179–186.
87. Rullo M, Cipolloni M, Catto M, Colliva C, Miniero DV, Latronico T, de Candia M, Benicchi T, Linusson A, Giacche N, et al. Probing fluorinated motifs onto dual AChE-MAO B inhibitors: rational design, synthesis, biological evaluation, and early-ADME studies. J Med Chem. 2022;65(5):3962–3977.
88. He Q, Liu J, Lan JS, Ding J, Sun Y, Fang Y, Jiang N, Yang Z, Sun L, Jin Y, et al. Coumarin-dithiocarbamate hybrids as novel multitarget AChE and MAO-B inhibitors against Alzheimer's disease: design, synthesis and biological evaluation. Bioorg Chem. 2018;81:512–528.
89. Pisani L, Iacobazzi RM, Catto M, Rullo M, Farina R, Denora N, Cellamare S, Altomare CD. Investigating alkyl nitrates as nitric oxide releasing precursors of multitarget acetylcholinesterase-monoamine oxidase B inhibitors. Eur J Med Chem. 2019;161:292–309.
90. Carradori S, Silvestri R. New frontiers in selective human MAO-B inhibitors. J Med Chem. 2015;58(17):6717–6732.
91. Gaspar A, Reis J, Fonseca A, Milhazes N, Vina D, Uriarte E, Borges F. Chromone 3-phenylcarboxamides as potent and selective MAO-B inhibitors. Bioorg Med Chem Lett. 2011;21(2):707–709.
92. Gaspar A, Silva T, Yanez M, Vina D, Orallo F, Ortuso F, Uriarte E, Alcaro S, Borges F. Chromone, a privileged scaffold for the development of monoamine oxidase inhibitors. J Med Chem. 2011;54(14):5165–5173.
93. Reis J, Cagide F, Estrada Valencia M, Teixeira J, Bagetta D, Perez C, Uriarte E, Oliveira PJ, Ortuso F, Alcaro S, et al. Multi-target-directed ligands for Alzheimer's disease: discovery of chromone-based monoamine oxidase/cholinesterase inhibitors. Eur J Med Chem. 2018;158:781–800.
94. Wang XB, Yin FC, Huang M, Jiang N, Lan JS, Kong LY. Chromone and donepezil hybrids as new multipotent cholinesterase and monoamine oxidase inhibitors for the potential treatment of Alzheimer's disease. RSC Med Chem. 2020;11(2):225–233.
95. Estrada-Valencia M, Herrera-Arozamena C, Perez C, Vina D, Morales-Garcia JA, Perez-Castillo A, Ramos E, Romero A, Laurini E, Pricl S, et al. New flavonoid – N,N-dibenzyl(N-methyl)amine hybrids: Multi-target-directed agents for Alzheimer ' s disease endowed with neurogenic properties. J Enzyme Inhib Med Chem. 2019;34(1):712–727.
96. Łażewska D, Bajda M, Kaleta M, Zaręba P, Doroz-Płonka A, Siwek A, Alachkar A, Mogilski S, Saad A, Kuder K, et al. Rational design of new multitarget histamine H-3 receptor ligands as potential candidates for treatment of Alzheimer's disease. Eur J Med Chem. 2020;207:112743.
97. Campora M, Canale C, Gatta E, Tasso B, Laurini E, Relini A, Pricl S, Catto M, Tonelli M. Multitarget biological profiling of new naphthoquinone and anthraquinone-based derivatives for the treatment of Alzheimer's disease. ACS Chem Neurosci. 2021;12(3):447–461.
98. Onoda M, Fujita K. Iridium-catalyzed C-alkylation of methyl group on *N*-heteroaromatic compounds using alcohols. Org Lett. 2020;22(18):7295–7299.
99. Xu R, Xiao G, Li Y, Liu H, Song Q, Zhang X, Yang Z, Zheng Y, Tan Z, Deng Y. Multifunctional 5,6-dimethoxybenzo[d]isothiazol-3(2H)-one-*N*-alkylbenzylamine derivatives with acetylcholinesterase, monoamine oxidases and β-amyloid aggregation inhibitory activities as potential agents against Alzheimer's disease. Bioorg Med Chem. 2018;26(8):1885–1895.
100. Liu Z, Shi Y, Zhang X, Yu G, Li J, Cong S, Deng Y. Discovery of novel 3-butyl-6-benzyloxyphthalide Mannich base derivatives as multifunctional agents against Alzheimer's disease. Bioorg Med Chem. 2022;58:116660.
101. Nadeem MS, Khan JA, Kazmi I, Rashid U. Design, synthesis, and bioevaluation of indole core containing 2-arylidine derivatives of thiazolopyrimidine as multitarget inhibitors of cholinesterases and monoamine oxidase A/B for the treatment of Alzheimer disease. Acs Omega. 2022;7(11):9369–9379.
102. Denya I, Malan SF, Enogieru AB, Omoruyi SI, Ekpo OE, Kapp E, Zindo FT, Joubert J. Design, synthesis and evaluation of indole derivatives as multifunctional agents against Alzheimer's disease. Medchemcomm. 2018;9(2):357–370.
103. Xu Y, Zhang J, Wang H, Mao F, Bao K, Liu W, Zhu J, Li X, Zhang H, Li J. Rational design of novel selective dual-target inhibitors of acetylcholinesterase and monoamine oxidase B as potential anti-Alzheimer's disease agents. ACS Chem Neurosci. 2019;10(1):482–496.
104. Osmaniye D, Evren AE, Saglik BN, Levent S, Ozkay Y, Kaplancikli ZA. Design, synthesis, biological activity, molecular docking, and molecular dynamics of novel benzimidazole derivatives as potential AChE/MAO-B dual inhibitors. Arch Pharm. 2022;355(3):e210045.
105. Tzvetkov NT, Stammler HG, Georgieva MG, Russo D, Faraone I, Balacheva AA, Hristova S, Atanasov AG, Milella L, Antonov L, et al. Carboxamides vs. Methanimines: crystal

structures, binding interactions, photophysical studies, and biological evaluation of (indazole-5-yl)methanimines as monoamine oxidase B and acetylcholinesterase inhibitors. Eur J Med Chem. 2019;179:404–422.
106. Karaca Ş, Osmaniye D, Sağlık BN, Levent S, Ilgın S, Özkay Y, Karaburun AÇ, Kaplancıklı ZA, Gundogdu-Karaburun N. Synthesis of novel benzothiazole derivatives and investigation of their enzyme inhibitory effects against Alzheimer's disease. RSC Adv. 2022;12(36):23626–23636.
107. Chimenti F, Bolasco A, Secci D, Chimenti P, Granese A, Carradori S, Yanez M, Orallo F, Ortuso F, Alcaro S. Investigations on the 2-thiazolylhydrazyne scaffold: synthesis and molecular modeling of selective human monoamine oxidase inhibitors. Bioorg Med Chem. 2010;18(15): 5715–5723.
108. Turan-Zitouni G, Hussein W, Sağlık BN, Tabbi A, Korkut B. Design, synthesis and biological evaluation of novel *N*-pyridyl-hydrazone derivatives as potential monoamine oxidase (MAO) inhibitors. Molecules. 2018;23(1):113.
109. Carradori S, Ortuso F, Petzer A, Bagetta D, De Monte C, Secci D, De Vita D, Guglielmi P, Zengin G, Aktumsek A, et al. Design, synthesis and biochemical evaluation of novel multi-target inhibitors as potential anti-Parkinson agents. Eur J Med Chem. 2018;143:1543–1552.
110. Tok F, Koçyiğit-Kaymakçıoğlu B, Sağlık BN, Levent S, Özkay Y, Kaplancıklı ZA. Synthesis.and biological evaluation of new pyrazolone schiff bases as monoamine oxidase and cholinesterase inhibitors. Bioorg Chem. 2019;84:41–50.
111. Vishnu MS, Pavankumar V, Kumar S, Raja AS. Experimental and computational evaluation of piperonylic acid derived hydrazones bearing isatin moieties as dual inhibitors of cholinesterases and monoamine oxidases. Chemmedchem. 2019;14(14):1359–1376.
112. Palakkathondi A, Oh JM, Dev S, Rangarajan TM, Kaipakasseri S, Kavully FS, Gambacorta N, Nicolotti O, Kim H, Mathew B. (Hetero-)(arylidene)arylhydrazides as multitarget-directed monoamine oxidase inhibitors. ACS Comb Sci. 2020;22(11):592–599.
113. Çevik UA, Osmaniye D, Sağlik BN, Çavuşoğlu BK, Levent S, Karaduman AB, Ilgin S, Karaburun AÇ, Özkay Y, Kaplancikli ZA, et al. Multifunctional quinoxaline-hydrazone derivatives with acetylcholinesterase and monoamine oxidases inhibitory activities as potential agents against Alzheimer's disease. Med Chem Res. 2020;29(6):1000–1011.
114. Saleem Khan M, Asif Nawaz M, Jalil S, Rashid F, Hameed A, Asari A, Mohamad H, Ur Rehman A, Iftikhar M, Iqbal J, et al. Deep eutectic solvent mediated synthesis of 3,4-dihydropyrimidin-2(1*H*)-ones and evaluation of biological activities targeting neurodegenerative disorders. Bioorg Chem. 2022;118:105457.
115. Jia Z, Wen H, Huang S, Luo Y, Gao J, Wang R, Wan K, Xue W. Click assembly of novel dual inhibitors of AChE and MAO-B from pyridoxine derivatives for the treatment of Alzheimer's disease. Heterocycl Commun. 2022;28(1):18–25.
116. Ye C, Xu R, Cao Z, Song Q, Yu G, Shi Y, Liu Z, Liu X, Deng Y. Design, synthesis, and in vitro evaluation of 4-aminoalkyl-1(2*H*)-phthalazinones as potential multifunctional anti-Alzheimer's disease agents. Bioorg Chem. 2021;111:104895.
117. Zhu G, Wang K, Shi J, Zhang P, Yang D, Fan X, Zhang Z, Liu W, Sang Z. The development of 2-acetylphenol-donepezil hybrids as multifunctional agents for the treatment of Alzheimer's disease. Bioorg Med Chem Lett. 2019;29(19): 126625.
118. Kosak U, Strasek N, Knez D, Jukic M, Zakelj S, Zahirovic A, Pislar A, Brazzolotto X, Nachon F, Kos J, et al. N-alkylpiperidine carbamates as potential anti-Alzheimer's agents. Eur J Med Chem. 2020;197:112282.
119. Guieu B, Lecoutey C, Legay R, Davis A, Sopkova de Oliveira Santos J, Altomare CD, Catto M, Rochais C, Dallemagne P. First synthesis of racemic trans propargylamino-donepezil, a pleiotrope agent able to both inhibit AChE and MAO-B, with potential interest against Alzheimer's disease. Molecules. 2020;26(1):80.
120. Nadeem MS, Khan JA, Rashid U. Fluoxetine and sertraline based multitarget inhibitors of cholinesterases and monoamine oxidase-A/B for the treatment of Alzheimer's disease: synthesis, pharmacology and molecular modeling studies. Int J Biol Macromol. 2021;193(Pt A):19–26.
121. Javed MA, Bibi S, Jan MS, Ikram M, Zaidi A, Farooq U, Sadiq A, Rashid U. Diclofenac derivatives as concomitant inhibitors of cholinesterase, monoamine oxidase, cyclooxygenase-2 and 5-lipoxygenase for the treatment of Alzheimer's disease: Synthesis, pharmacology, toxicity and docking studies. RSC Adv. 2022;12(35):22503–22517.